The Unfolding Action Model of Initiation Times, Movement Times, and Movement Paths

Cristian Buc Calderon
Ghent University and Université Libre de Bruxelles

Wim Gevers
Université Libre de Bruxelles

Tom Verguts
Ghent University

Converging evidence has led to a consensus in favor of computational models of behavior implementing continuous information flow and parallel processing between cognitive processing stages. Yet, such models still typically implement a discrete step between the last cognitive stage and motor implementation. This discrete step is implemented as a fixed decision bound that activation in the last cognitive stage needs to cross before action can be initiated. Such an implementation is questionable as it cannot account for two important features of behavior. First, it does not allow to select an action while withholding it until the moment is appropriate for executing it. Second, it cannot account for recent evidence that cognition is not confined prior to movement initiation, but consistently leaks into movement. To address these two features, we propose a novel neurocomputational model of cognition-action interactions, namely the unfolding action model (UAM). Crucially, the model implements *adaptive information flow* between the last cognitive processing stage and motor implementation. We show that the UAM addresses the two abovementioned features. Empirically, the UAM accounts for traditional response time data, including positively skewed initiation time distribution, functionally fixed decision bounds and speed–accuracy trade-offs in button-press experimental designs. Moreover, it accounts for movement times, movement paths, and how they are influenced by cognitive-experimental manipulations. This move should close the current gap between abstract decision-making models and behavior observed in natural habitats.

Keywords: action selection, decision-making, adaptive information processing, neurocomputational model, reaching task

Humans rely on their ability to select relevant actions in order to survive. For instance, some indigenous tribes rely on precise hunting techniques such as spear fishing to feed. When multiple preys are afforded by the environment, spear fishing constitutes an action selection problem. Understanding the underlying cognitive processes and neural mechanisms involved in resolving this selection problem has been the attentional focus of cognitive (neuro) science and psychology of decision-making for more than four decades. To that endeavor, scientists have proposed a wide variety of computational models in distinct research domains such as language (Spivey, Grosjean, & Knoblich, 2005), numerical cognition (Dotan & Dehaene, 2016), reinforcement learning (Daw, Niv, & Dayan, 2005), working memory (Oberauer, Souza, Druey, & Gade, 2013), semantic processing (Ralph, Jefferies, Patterson, & Rogers, 2017), metacognition (Fleming & Daw, 2017), and cognitive control (Botvinick, Braver, Barch, Carter, & Cohen, 2001), to cite but a few. In the following, we briefly review the theoretical and architectural evolution of such computational models. Subsequently, we point out a *cognition-action gap* that is problematic in such models. Finally, we propose a novel computational model overcoming this issue while still accounting for the most prominent behavioral features accounted for by previous models.

Strict Serial Processing

Perhaps the first explicit model architecture for cognitive processing was proposed in the pioneer work of Donders (1868, 1969). The author assumed that there are distinct, sequentially activated, information processing stages between perceiving a stimulus and producing a response. In this model, the output of one processing stage is taken as the input to the next, without any temporal overlap between the two stages. This process continues until a response is selected and implemented. Donders also devised a method to test (properties of) this strict serial stage model. In particular, his subtractive method allowed him to calculate the time needed for specific processing stages. Consider two tasks differing in only one processing stage. A first task involves pressing a button with the right index whenever the letter "i" appears in a flow of sequentially presented letters. A second task involves pressing a button with the right and left index whenever the letter "i" and "e" appear, respectively. Arguably, the second task contains an additional action selection processing stage compared to the first task. Hence, by subtracting the time associated to the first task from that of the second task, Donders suggested one could compute the time associated to the additional processing stage (i.e., action selection).

The subtractive method came under criticism. It seemed inconceivable to design experimental tasks that would uniquely add or remove a specific processing stage without influencing the other processing stages. Following the same serial architecture, Sternberg suggested an alternative approach, the additive method, to investigate the components of the strict serial stage model (Sternberg, 1969). He proposed that when experimental factors only target a specific processing stage (rather than influencing several ones), their effects on reaction times (RTs) would be independent and additive. Sternberg's approach had the advantage that it did not require adding or removing specific components (stages) in the serial processing stream.

The strict serial stage information processing model and accompanying additive method were soon applied in several areas of cognition including reading (McCusker, Gough, & Bias, 1981), memory (Sternberg, 1966), problem solving (Simon & Newell, 1971), numerical cognition (Capaldi & Miller, 1988), and vision (Marr, 1976). For instance, early work in reading (e.g., Gough, 1972) suggested that each letter would be separately and serially encoded into phonemes. Once encoded, these phonemes would then be tied together to form individual words. The idea of cutting up general information in different pieces to be independently and serially processed was translated to brain functioning as well. A modular view of the brain was developed where each processing stage/module within a serial processing stream would be subtended by a distinct brain area (e.g., Fodor, 1983). Broadly speaking, perceptive processes would be subtended in visual occipital areas, cognitive processes in high-order associative cortices (i.e., fronto-parietal networks), and the output of the final cognitive stage (e.g., action selection), would be sent to the motor areas, which execute the action (Keele, 1968; Miller, Galanter, & Pribram, 1960).

In sum, strict serial processing is encapsulated by two main features. First, seriality: processing stages are arranged in a chain. Second, thresholding: a processing stage needs to be completed before the subsequent stage starts. A cornerstone argument in favor of a processing architecture implementing these two features emanates from the seminal serial search paradigm. In this paradigm, participants have to report whether a target symbol is present in a previously memorized sequence of symbols. Typically, mean RT linearly increase as a function of the sequence length (e.g., Sternberg, 1966). It was concluded that only a model architecture composed of serially arranged comparison processing stages (i.e., seriality), whereby each symbol in the memorized sequence is compared to the target symbol one at a time (i.e., thresholding), could explain such a linear RT function.

Computational Advances and Alternative Accounts

The strict serial stage model was soon criticized by two main novel processing insights. First, instead of implementing thresholding between the distinct processing stages, it was suggested that information may directly leak from each stage to the subsequent one in the serial chain. Such a continuous flow is at the heart of the cascade model of McClelland (1979). In particular, that model suggests that every processing unit belonging to a specific stage continuously feeds information to the processing unit(s) it is connected to in the subsequent stage. The connections from the penultimate cognitive stage project to a final cognitive stage where two (or more) responses, corresponding to each potential choice in the task at hand, compete for being executed by the subsequent motor stage. Importantly, McClelland (1979) demonstrated that the additive logic of Sternberg (1969) could be applied under specific circumstances to networks arranged in cascade. This type of information processing was also suggested by Eriksen and Schultz (1979) to take place in visual search tasks, and was designated as a continuous flow conception.

Second, an even more compelling blow to serial stage processing followed directly on the serial search paradigm. In particular, rigorous mathematical theorems proved that limited capacity parallel processing models were not only perfectly able to mimic the linear RT curves suggested to stem from serial processing, but also systematically provided better fit to the data (Townsend, 1972, 1976, 1981). Further work (Townsend, 1990) also discussed the importance of disentangling between serial and parallel processing, and proposed different methods to do that.

The architecture debate was born and, based on these computational advancements, novel models saw the light. Broadly speaking the resulting models can be situated on a two-dimensional space where the first dimension, the *information flow* dimension, defines whether the information flow between stages is continuous or thresholded; and the second dimension, the *architecture* dimension, defines whether the processing stages are arranged in serial chain or in parallel. For instance, in the seminal work of Quillian (1967, 1969) semantic processing results from automatic spreading activation between processing units, each coding for one concept, that form an interconnected (i.e., not serially chained) network. Here, the concept represented by a specific unit is not fully processed when activation is passed to another unit (representing another concept). Thereby, such a model would be defined by continuous information flow and parallel processing stages (also see Collins & Loftus, 1975).

Consensus and Remaining Issues

Influential models have been associated to distinct locations in this two-dimensional space. Nonetheless, a consensus has gradu-

ally been reached in favor of models implementing both continuous information flow and a parallel architecture. These models have found support in studies using neurophysiological as well as imaging techniques. Supporting parallel architecture, single-cell recording studies in nonhuman primates have consistently shown that processing channels representing each potential action in the task at hand are activated in parallel (Cisek, 2006; Cisek & Kalaska, 2005; Klaes, Westendorff, Chakrabarti, & Gail, 2011). Supporting continuous information flow, using magnetoencephalography (MEG), it has been shown that the competition between potential action plans in a perceptual decision task is biased from the very beginning all the way up to the primary motor cortex (e.g., Donner, Siegel, Fries, & Engel, 2009). Furthermore, several studies have shown that representations of potential action plans in (pre)motor cortices (Bastian, Schöner, & Riehle, 2003; Michelet, Duncan, & Cisek, 2010; Thura & Cisek, 2014), are biased by decision variables such as reward from the very beginning of the decision process (Lauwereyns, Watanabe, Coe, & Hikosaka, 2002).

However, despite their advantages, current models have two questionable properties in common. First, information flow from one stage to another is typically *nonadaptive*. Note that this is the case both for continuous (e.g., cascade model) and thresholded information flow (e.g., serial stage model) systems. Continuous information flow corresponds to a zero threshold, and thresholded information flow corresponds to a nonzero, but constant threshold value. This property will from now on be called *unadaptive information flow*. Hence, these models do not allow for an adaptive information flow between processing stages. Yet, this is essential for optimal functioning. Consider again the spear fishing action selection problem. It is key for a successful spear shooter to withhold the action until the moment is optimal to hit the prey. This implies a system that can select an action but withhold it if the moment is not optimal, that is, separating what action to select from when to execute it. Hence, we propose to add a third level to the information flow dimension, namely *adaptive information flow*. This level allows implementing a break on a continuous flow of information, thereby loading cognitive information and releasing it upon the optimal moment (i.e., separating what to do from when to do it).

Second, current models typically assume that information flow between the final cognitive and the motor stage is thresholded, that is, action is only initiated when cognition is fully finished. This property, from now on called *cognition-action thresholding*, is present in all models discussed up to now. Cognition-action thresholding is implemented also in the cascade model (cfr. Figure 1 in McClelland, 1979), and has been repeatedly implemented in more recent continuous information flow models in distinct domains such as, numerical cognition (Gevers, Verguts, Reynvoet, Caessens, & Fias, 2006), cognitive control (Botvinick et al., 2001), task switching (Gilbert & Shallice, 2002), and task set learning and generalization (Collins & Frank, 2013). Moreover, cognition-action thresholding is also a key feature in accumulation-to-bound models (Cisek, Puskas, & El-Murr, 2009; Ratcliff, 1978; Ratcliff & Rouder, 1998), where action is initiated only when evidence in favor of a specific response reaches a (fixed or collapsing) decision threshold.

One reason why cognition-action thresholding has been implemented even in continuous information flow models is that such thresholding has received support from neurophysiological studies. In monkeys, the firing rate of motor neurons encoding for potential actions reaches a fixed rate at the moment of the decision, irrespective of task difficulty, which is suggestive of cognition-action thresholding (Gold & Shadlen, 2007; see also Churchland, Kiani, & Shadlen, 2008; Roitman & Shadlen, 2002; Schall & Bichot, 1998; Thura & Cisek, 2014). In humans, Twomey, Murphy, Kelly, and O'Connell (2015) reported that the P300 (an event-related EEG potential peaking around 300 ms–600 ms after task-relevant stimulus onset) reaches a fixed amplitude just prior to response execution, again irrespective of task difficulty (see also Murphy, Robertson, Harty, & O'Connell, 2015; O'Connell, Dockree, & Kelly, 2012). However, cognition-action thresholding seems incompatible with recent theoretical accounts, based on extensive behavioral and neurophysiological evidence (see below), suggesting that behavior stems from a continuous information flow involving perceptual, cognitive and motor processes (e.g., Magnuson, 2005). Indeed, by definition, cognition-action thresholding impeaches cognitive processes and motor processes to overlap in time. Computational models should be able to account for those effects of cognition on ongoing actions. Interestingly, as described later on, adaptive information flow between the final cognitive and the motor stage has the potential to account both for the emergence of thresholded information flow between cognition and action, as well as the continuous overlap between cognitive and motor processes.

Neural and Behavioral Evidence Supporting Adaptive Information Flow and Temporal Overlap Between Cognition and Action

Adaptive information flow would implement a brake on the information processing flow in order to separate what action to perform from when to perform it, or more generally, for allowing information to flow from one stage to another at the right time. Interestingly, recent studies suggest that adaptive information flow may be supported by the subthalamic nucleus (STN; Frank, 2006; Weintraub & Zaghloul, 2013). For instance, rats with STN lesions have difficulties estimating when to perform a relevant action and thereby display compulsive lever-pressing for reward (Winter et al., 2008). Moreover, lesions to the STN induce premature responding (Baunez et al., 2001; Baunez & Robbins, 1997). Deep brain stimulation (DBS) in STN increases speed and decreases accuracy in tasks inducing choice conflict (e.g., Stroop Task; Jahanshahi et al., 2000). Also with DBS, Cavanagh et al. (2011) showed that when stimulating the STN (disrupting its functional role), patients with Parkinson's disease displayed impulsive choices in highly conflictual situations. In the same vein, using fMRI and a stop-signal task, Aron and Poldrack (2006) observed that successful stops significantly activated the STN. Altogether, these studies suggest that the STN may implement a break on information flow in order for the system to resolve response conflict prior to allowing information to flow in the subsequent motor stage. Importantly, the STN receives anatomical inputs from several motor areas (directly from primary motor cortex, Alexander & Crutcher, 1990; indirectly from preSMA; Aron et al., 2007). Furthermore, it projects back to motor areas (via pallidum and thalamus). Therefore, STN might pick up (pre-)motor cortex signals in order to gate motor cortex in a negative feedback loop, thus

separating what to do from when to do it (i.e., implementing adaptive information flow). This is known as the STN hypothesis (Forstmann et al., 2010).

We further suggest that cognitive and motor processes overlap in time. Such a proposal is supported by several reaching task studies providing novel insights into the information processing nature of the final processing stages. For instance, action selection (cognitive) processes are not confined prior to movement initiation (action) but rather continuously influence motor processes, thereby suggesting parallel activation between cognitive and motor processes (Boulenger et al., 2006; Calderon, Dewulf, Gevers, & Verguts, 2017; Calderon, Verguts, & Gevers, 2015; Chapman et al., 2010; Cressman, Franks, Enns, & Chua, 2007; Resulaj, Kiani, Wolpert, & Shadlen, 2009; Santens, Goossens, & Verguts, 2011; Sullivan, Hutcherson, Harris, & Rangel, 2015). For instance, Chapman and colleagues (2010) observed that reach trajectories are more attracted toward the side of a display when it contains more potential targets compared with the opposite side. This reach trajectory attraction bias is suggested to stem from an unbalance (in favor of the side containing more potential targets) of simultaneously activate reach plans.

Implementing Adaptive Information Flow

Both questionable properties raised above (i.e., unadaptive information flow and cognition-action thresholding) can be dealt with by implementing adaptive information flow between the last cognitive and motor stage. With this in mind, we developed a neurocomputational model of cognition-action interactions. In the initial phases of cognitive processing, the model inhibits actions depending on contextual constraints. Actions do not start when activity crosses a fixed threshold: Rather, actions start to be implemented once a dynamically modifiable inhibition level is sufficiently surpassed. Thus, the issue associated with unadaptive information flow (i.e., separating what to do from when to do it) is addressed. When this dynamic threshold is crossed, no "motor stage" is initiated; cognitive processing simply continues, but it now has motor consequences. Thus, the issue of cognition-action thresholding (i.e., cognition leaks into action) is addressed.

The model is illustrated in three simulations. In Simulation 1, we consider model performance in the most widely used task to study decision making models, namely the two-alternative forced choice (2AFC) task. The model can account for the typical behavioral results such as RT distributions and speed–accuracy trade-offs (Bogacz, Wagenmakers, Forstmann, & Nieuwenhuis, 2010). We further show that our model (implementing adaptive information flow between the last cognitive and the motor stage) accounts for data that was interpreted as favoring thresholded information flow (i.e., fixed decision bound) between cognition and action. To strengthen this point we extract parameters from the drift diffusion model (DDM; Vandekerckhove & Tuerlinckx, 2008) on the simulated data in order to interpret the model's functioning. In Simulation 2, we demonstrate that our model can account for the effects of cognition on unfolding actions. Specifically, we show that our model can account for the initiation times (ITs), movement times (MTs), and movement paths in reaching tasks (e.g., Calderon et al., 2015). In Simulation 3, we generalize the effect of a cognitive manipulation to a completely different domain, namely numerical cognition (Santens et al., 2011).

The Unfolding Action Model (UAM)

The UAM architecture is illustrated in Figure 1A. An input layer projects to dorsal premotor cortex (PMd). The latter currently consists of two response options (left [L] and right [R] target direction), in line with the experiments we will model. In turn, the PMd layer has ipsilateral excitatory connections with the primary motor (M1) layer. Competition between reach target directions is implemented within both the PMd and M1 layer through lateral inhibition (e.g., Duque et al., 2007). Hence, our model displays a parallel architecture instantiated by two parallel processing channels representing two concurrent potential action plans. Each processing channel is composed of distinct processing stages. The M1 layer projects to a movement vector layer (presumably located in brainstem or spine; see General Discussion section); and movement trajectory is implemented as a continuously updated M1-activity-weighted vector addition (Figure 1A). Finally, M1 also projects to the STN (Alexander & Crutcher, 1990), implementing a negative feedback loop for M1. In particular, STN functions as an adaptive gate for movement execution that is modified online depending on M1 dynamics. Specifically, as the activation difference between M1 processing units increases, so does the width of the movement execution gate (see Figure 1B, C). Hence, information flow is continuous up until M1. However, information flow between M1 (i.e., the last cognitive stage) and motor stage is adaptive; and this adaptive information flow is gated by the STN. Full mathematical implementation of the UAM (and biological motivation) can be found in Appendix A.

Simulation 1: Decision Making

The movement vectors can be chosen such as to implement any desired task-specific movement parameters (see Method section below). A straightforward example would be a button press task: In the current framework, a button press task is just a task requiring short movement vectors. We thus start our simulation series by investigating whether the UAM accounts for extant data in the staple of experimental psychology, the two-alternative forced-choice (2AFC) task of decision making. Specifically, two model aspects were investigated in this simulation. The first is positive skew. RTs virtually always have a positively skewed distribution (Luce, 1986). This is therefore a first feature that any plausible model of RTs (or ITs) must adhere to. Second, faster RT often comes with an accuracy cost. This effect is known as the speed–accuracy trade-off (SAT; Bogacz et al., 2010). Depending on the environmental constraints, agents can optimally set this tradeoff to either emphasize speed or accuracy (Heitz, 2014). We thus also investigated whether the UAM accounts for SAT. For this purpose, two data sets were simulated, one with a high (emphasizing accuracy) and one with a low (emphasizing speed) STN initial value (Figure 2C). As extensively described below, our adaptive information flow implementation also explains the emergence of thresholded information flow (i.e., fixed decision bound). Specifically, modifying the STN initial value has a direct influence on adaptive information flow, and thereby on the emergence of thresholded information flow. A high STN initial value will induce a conservative information flow threshold (high decision bound), that will in turn induce slow but accurate RTs. Conversely, a low STN initial value will induce a low information flow threshold (low decision bound), that will in turn induce fast but error prone RTs.
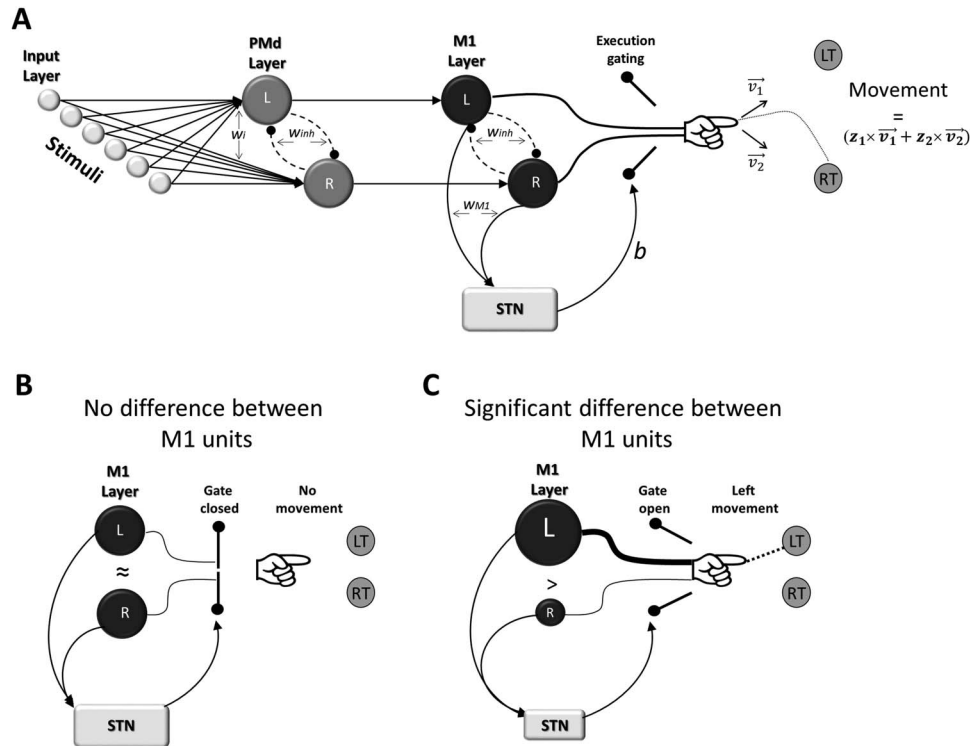
Figure 1. Model Outline. (A) Neural architecture. The model consists of input, dorsal premotor, primary motor layers and STN. The input layer projects onto the PMd layer. In turn the PMd layer projects to the M1 layer. The M1 layer projects to the STN that picks up a signal of the difference in activation value between the M1 processing units (i.e., M1 dynamics). Depending on the M1 dynamics, the STN either opens or closes the gate for movement. Movement is represented as a weighted (by M1 activation) vector addition that is continuously updated. (B) Inhibition and STN function. The activation difference of M1 units is small. Here, movement is inhibited. (C) Movement and STN function. When activation increases in a unit relative to the other (i.e., when the biased competition favors a particular action plan, here the left movement plan), the STN value decreases and it inhibits less, to the point that movement is gradually released. LT = left target; RT = right target.

Method

Design. We simulate a generic 2AFC task where Stimulus 1 and 2 require a left and a right button press, respectively (see Figure 2A). Examples of stimuli would be arrows pointing left or right (Boy, Husain, & Sumner, 2010), random dots moving left or right (Shadlen & Newsome, 2001), or words and nonwords (Meyer & Schvaneveldt, 1971). Stimulus 1 and 2 activate input unit 1 and 2, respectively, which then activate PMd. Errors in simulated ITs occur when the activity of the irrelevant M1 unit displays a higher activity than the relevant M1 unit once a response is given. Depending on the stimulus (i.e., left or right arrow), one specific input unit was active at a time ($x_i = 1$).

Data analysis. Two data sets of 4,000 trials were simulated (2,000 for each stimulus) for each condition (i.e., emphasizing speed or accuracy). Parameter values are displayed in the Appendix B. To test for positive skew, we plotted the IT distributions and calculated Pearson's moment coefficient of skewness (γ) for each simulated data set. A value of 0 indicates a perfectly symmetrical distribution, a negative value indicates a negative skew distribution, and a positive value indicates positive skew. To test for the SAT, the accuracy in each simulated data set was calculated and their IT distributions were plotted.

To further investigate the role of STN functionality in our model, we fitted the diffusion model (DDM; Ratcliff, 1978) to the simulation data. The DDM explains performance in 2AFC tasks through a sequential evidence accumulation process over time. Of specific interest are two parameters of the DDM, namely the decision bound a and the drift rate v. The decision bound defines how much evidence is needed to make a choice, and the drift rate defines the speed of evidence accumulation. We reasoned that because the STN gates action execution (i.e., choice implementation), ITs simulated with two distinct STN initial levels should best be accounted for by a DDM allowing the decision bound to vary freely across conditions. We therefore tested four models (all combinations of a and v free or fixed) using the Diffusion Model Analysis Toolbox (DMAT; Vandekerckhove & Tuerlinckx, 2008).

Response implementation. Movement is implemented through a M1-activity-weighted vector addition. Specifically, the vector associated to a left response (i.e., $\vec{v_1} = \begin{bmatrix} -1 \\ +1 \end{bmatrix}$) is weighted by the activation value of the left M1 unit (z_1), and the vector associated to a right response (i.e., $\vec{v_2} = \begin{bmatrix} +1 \\ +1 \end{bmatrix}$) is weighted by the activation value of the right M1 unit (z_2). In turn, once the action gate opens, movement is defined by the following differential equation:
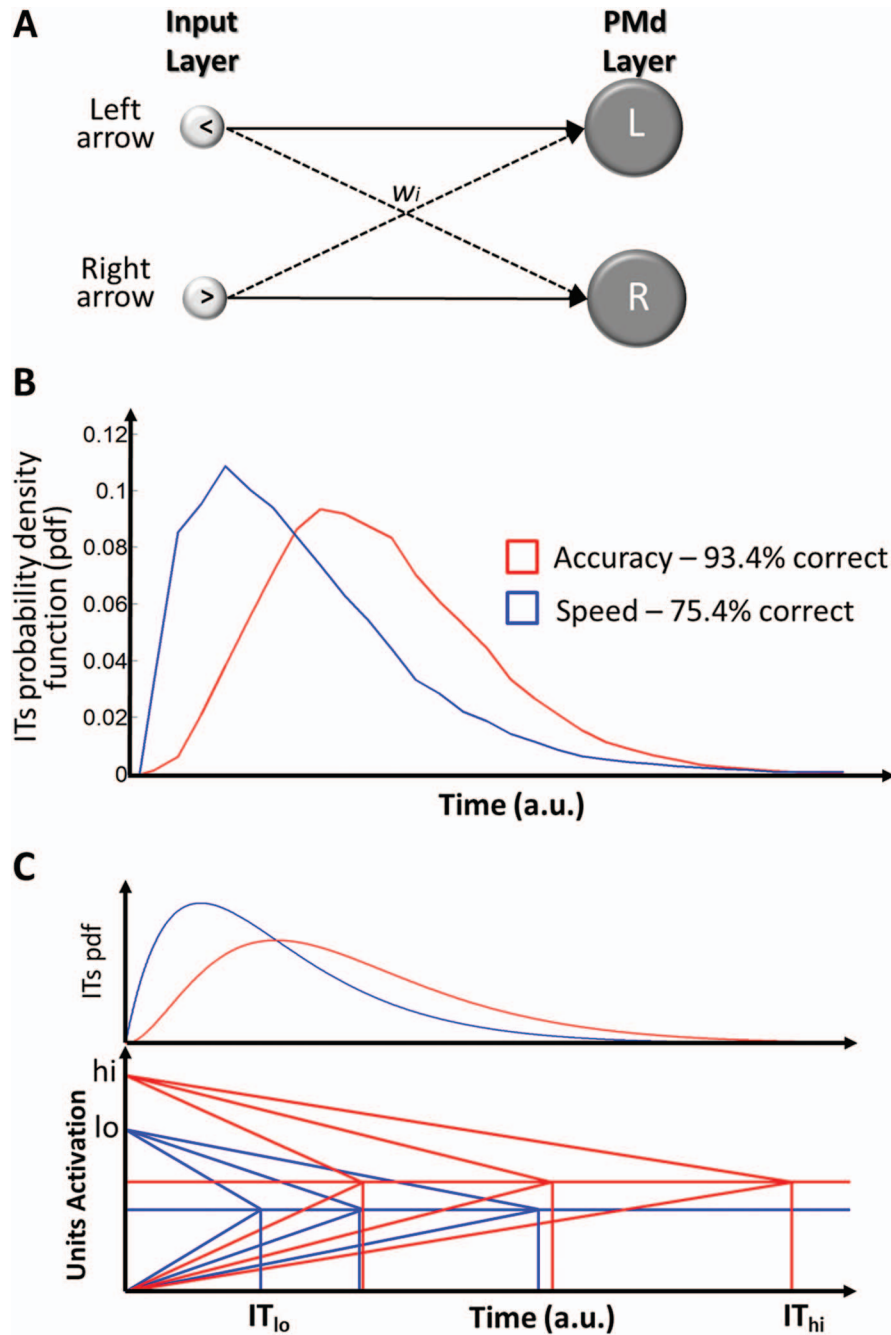
Figure 2.   Simulation 1, 2AFC Task. (A) Mapping used in the 2AFC task. Each stimulus is connected to the PMd layer unit with a certain weight. In this case, arrow stimuli fully determine the required response. Therefore, a left arrow stimulus is connected with a weight w = 0 (i.e., dashed line) to the right PMd unit and a weight w = 1 (i.e., plain line) to the left PMd unit (same logic applies to a right arrow). (B) Two simulated RT distributions. The red and blue distribution corresponds to the output of a model emphasizing accuracy and speed, respectively. A high initial STN value (red distribution) induces slower ITs and high accuracy. In contrast, a low initial STN value (blue distribution) produces faster ITs and low accuracy. (C) Illustration of positive skew, speed–accuracy trade-off and thresholded information flow (fixed decision bound). The level lo on the ordinate represents the STN initial value when speed is favored over accuracy (blue lines). The level hi on the ordinate illustrates the STN initial value when accuracy is emphasized (red lines). See text for detailed explanation of the model predictions regarding behavioral results of 2AFC tasks. Horizontal red and blue lines represent the activation value of the relevant motor unit at action initiation onset. Vertical red and blue lines represent the different ITs. The IT subindices represent whether they belong to the speed (lo) or accuracy (hi) condition. See the online article for the color version of this figure.

$$\frac{d}{dt}V(t) = (z_1 \times \vec{v_1} + z_2 \times \vec{v_2}) \qquad (1)$$

where z represents the activity of M1 units (see Appendix A). Thus, from an UAM perspective, a button press can be considered as a movement with small absolute size. The ITs were computed as the time interval between the input onset of the go signal and the moment that the vertical-dimension value of the movement (V) vector was >1.

Results

Figure 2B shows the IT distributions of the two simulated data sets, one emphasizing speed (blue) and the other accuracy (red); here and elsewhere, (initiation) time is measured in arbitrary units (a.u.). Both distributions have a positive skew, and skewness is enhanced in the speed-emphasis condition ($\gamma = 1.29$) relative to the accuracy-emphasis condition ($\gamma = 0.77$).

Second, the model with higher initial STN was indeed more accurate than with lower initial STN (93% and 75%, respectively), but slower (mean RT .77 and .41, respectively). Thus, the model implements speed–accuracy trade-off (SAT). This is further illustrated in Table 1, which shows the results (parameter estimates of a and v, and Bayesian Information Criterion (BIC) of the DDM fitting procedure for the four models considered above. Note that BIC automatically incorporates the effects of both fit and model complexity. The worst model is the one where no parameters are allowed to change across conditions. Second is the model where only drift rates can change. As predicted, the two best models are the ones where boundaries can change. Unexpectedly, the model with both free decision bound and free drift rate is the best of all. However, the free drift rate in the latter model is misleading because the drift rate estimates are in the opposite direction as predicted. One would expect the drift rate to increase when speed is emphasized; in contrast, the drift rate decreased when speed was emphasized. The decision bounds are in the expected direction: Decision bound is lower when speed is emphasized. Altogether, these results demonstrate that STN in our model approximates the DDM decision bound. This implies that the adaptive information flow instantiated in our model between M1 processing stages and motor implementation is a mechanism that can account for a large corpus of neurophysiological studies (e.g., Gold & Shadlen, 2007; Twomey et al., 2015) that have until now been taken as evidence for thresholded information flow in the last processing stage.

Discussion

The UAM exhibits two classical RT effects, namely positive skew and SAT. To understand why the model exhibits these effects, consider a cartoon of the model dynamics in Figure 2C, the blue lines in particular. Descending lines correspond to STN and ascending lines to the response-relevant motor processing unit. Each pair of touching lines (touching at the blue horizontal line) corresponds to a specific trial. The slopes of the ascending lines represent evidence strength for the relevant response. Steepness is subject to trial-by-trial variance, and when the slopes are steep, evidence in favor of the relevant response is strong. First, the geometric intuition explains why skew must be positive; there is simply more "room" for lines to cross on the right than on the left. Second, it's also clear from Figure 2C how the model can account for the SAT: By increasing the initial value of STN (red lines in Figure 2C), response and STN trajectories cross later, and this slows RT, increases accuracy, and decreases positive skew.

Adaptive information flow implementation also explains the emergence of thresholded information flow (i.e., fixed decision bound; see Gold & Shadlen, 2007). Let us focus on a given accuracy context (e.g., red lines in Figure 2C). In the UAM, the value of the STN linearly decreases (red descending lines) as a function of M1 unit activation (red ascending lines). In particular, a steep evidence accumulation increase (e.g., easy task with strong motion coherence) induces a steep STN value decrease. It follows that, for any given trial difficulty, the ascending and descending lines will cross around the same location on the ordinate, and therefore action initiation will begin once motor evidence accumulation reaches a specific value (red horizontal line; i.e., the action initiation threshold). This is true for any given STN initial value (see blue horizontal line in Figure 2C).

Simulation 2: Cognitive Control

To address both the leakage of cognitive processes into movement and the emergence of a fixed decision bound, we next consider a task where movement paths (MPs) can be studied. For this purpose, we used the reaching task of Calderon et al. (2015). In this task, participants had to reach toward the correct response target side (see Figure 3). Task difficulty was defined by a cue-target congruency; the cue could point in the same direction as the target (congruent, easy trial) or in the opposite direction (incongruent, difficult trial). It was found that the difficulty manipulation was observed both in ITs, as well as in the MTs and MPs. Hence, these results are in line with the view that cognitive processes influence motor processes after movement initiation (i.e., cognition leaking into movement). First, we test whether the UAM can also account for the difficulty manipulation not only at the level of ITs, but also MTs and MPs. Furthermore, the difficulty manipulation allows us to consider again, from an adaptive information flow perspective, the emergence of a fixed decision bound.

Table 1
DDM Fitting Results

Models	a – STN low	v – STN low	a – STN high	v – STN high	BIC
No effect	.179	.188	.179	.188	31760.51
Drift rate	.184	.323	.184	.176	31332.88
Decision bound	.139	.187	.216	.187	29268.26
Drift rate and decision bound	.149	.193	.364	.462	28846.09

Note. a = decision bound level; v = drift rate; STN low = initial level of the subthalamic nucleus of .5; STN high = initial level of the subthalamic nucleus of 1.2; DDM = drift diffusion model; BIC = Bayesian Information Criterion.
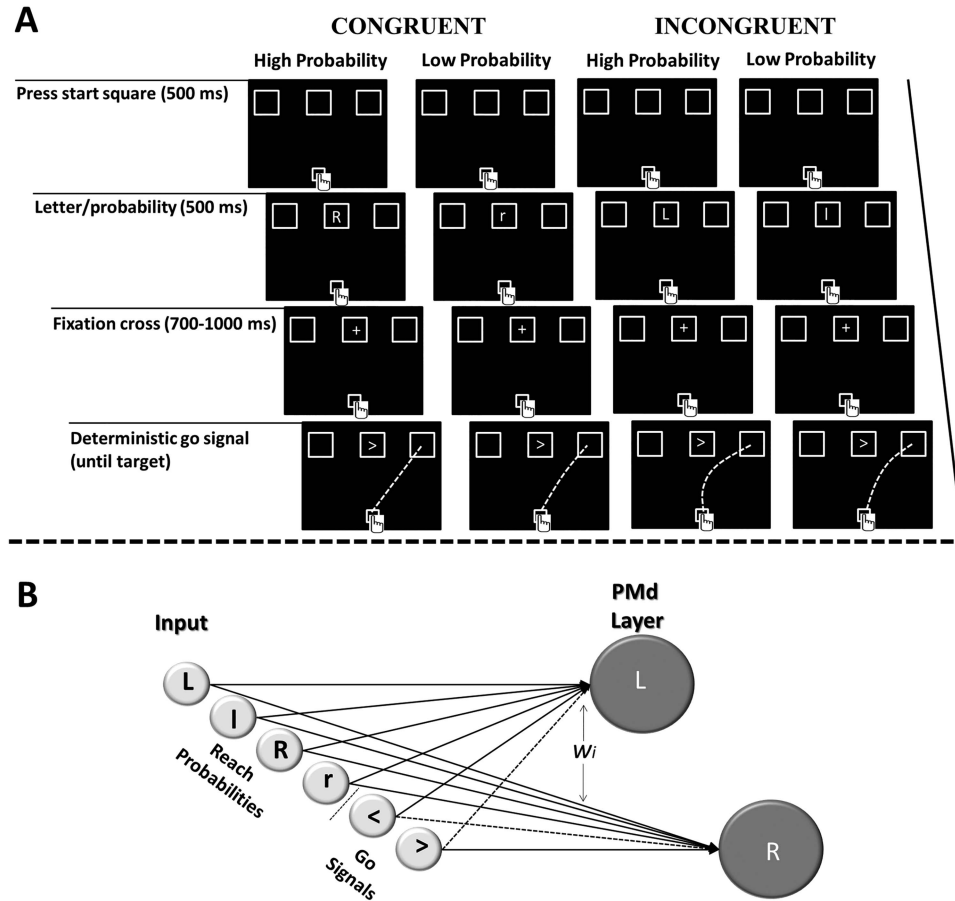
Figure 3. Simulation 2 Outline. (A) Experimental task design of Calderon et al. (2015). Participants first pressed the start square. Subsequently, they were shown a letter conveying the probabilities associated with each upcoming reach possibility. R and r represent, respectively, 80%/60% and 20%/40% for right/left reach probabilities (similar logic applies to L and l). Participants then saw a fixation cross followed by the go signal indicating them where to reach for. Depicted on the figure are two congruent and incongruent trials. For congruent trials, the side with the highest probability to be reached was the same side indicated by the arrow go signal. This pattern was reversed for incongruent trials. Moreover, trials could either have a high (uppercase letter) or low (lowercase letter) probability of being congruent or incongruent. Hence, cue-target congruency could either be of high or low probability. The dashed trajectories on the figure represent the hypothesized trajectories under each condition. (B) Mapping used in Simulation 2. Each stimulus is connected to the PMd layer unit with a certain weight (see Appendix C for input-PMd weight values).

As previously mentioned, EEG markers of sensorimotor activity (i.e., the amplitude of the P300 ERP) reached a fixed threshold regardless of trial difficulty (O'Connell et al., 2012). Second, we thus test whether this property also holds in the UAM.

Method

Design. Each trial started with a predictive cue regarding upcoming reach possibilities, before the target stimulus. Cues could either be congruent or incongruent with the upcoming target direction. Also, this cue-target congruency could either be of high probability (80%) or low probability (60%). ITs were computed as the time between the onset of the go signal (indicating which target to reach for) and the first data point falling outside a small start square location (that needed to be touched to start the trial). MTs

were defined as the time interval between leaving the start location and reaching the target location. Therefore, our experimental data conformed to a 2 (cue-target congruency; Congruent or Incongruent) $\times$ 2 (Probability; high or low) design; and for each cell we had an IT and MT. This provided us eight response time measures. Moreover, MPs corresponded to the horizontal and vertical locations of the movement during the MT. We predicted that task difficulty (implemented via the predictive task-relevant cues) would be revealed in ITs, MTs, and MPs (for details see Calderon et al., 2015).

We simulated 4,000 trials with an identical trial distribution as in Calderon et al. (2015). To match the sample size of Calderon et al. (2015) we simulated the MPs for 20 simulated participants. Input unit weights w_i are shown in Appendix C. As in the previous

simulation, one specific input (i.e., probability cue or go signal) unit was active at a time.

Data analysis. Because we now also fit MTs, we fitted the UAM rather than the diffusion model. The fitting procedure as well as best fit parameters are displayed in the Appendix B. After data fitting, response times are expressed in ms rather than in arbitrary units; for these and all subsequent analyses, all simulated ITs under 100 ms are discarded from the analyses.

In a next step, to test model robustness, we calculated the coefficient of determination (R^2; see fitting procedure) between our simulated (400 trials) and empirical data for distinct combinations of parameter values (as in Verguts, Vassena, & Silvetti, 2015). For the initial value of STN we took values ranging from 1.05 to 2 (steps of 0.1). For the decay parameter α, values ranged from 0.45 to 1.45 (steps of 0.05). Finally, for the encoding time α we took values ranging from 47 to 57 (steps of 1). We then created R^2 heatmaps by fixing each combination of two parameters and averaging across all values of the third parameter (see model fit and robustness below).

Response implementation. In Calderon et al. (2015), the IT was the time interval between the go signal onset and the moment when the vertical-dimension value of the online registered reach location crossed a certain level on the touchscreen, that is, the upper boundary of a start location square. MT was the time interval between crossing the upper boundary of the start location square and reaching the target location. Therefore, the ITs of the model were computed as the time interval between the input onset of the go signal and the moment that the vertical value of the movement (V; see Equation 1 above) vector was >1. To compute MTs, we calculated the time interval when the absolute values of the vector dimensions were respectively between 1 and 20 for the horizontal dimension, and between 1 and 50 for the vertical dimension. These values were chosen with respect to the target display in our previous study (i.e., the vertical reach distance reach was longer than the horizontal reach distance). To ensure that our simulated MPs end up at the same location, the reported MPs are normalized relative to their end point both for the lateral deviation (horizontal dimension) and reach distance (vertical dimension). Specifically, for all reaches, each data point on the two dimensions was divided by the maximal value on their respective dimension and multiplied by a constant (20 and 50 for the horizontal and vertical dimensions, respectively). Note that this manipulation does not distort the qualitative pattern of MPs.

Results

Initiation times. The result of our experimental manipulation on ITs is illustrated in Figure 4A. As can be seen, we first observed a congruency effect. Probability cues indicating the same side as the go signal (e.g., "R" followed by ">") yield faster ITs. Second, this congruency effect interacted with the level of probability (i.e., high or low). For congruent cue-target combinations, high probability cues induced faster ITs than low probability cues. This pattern reversed for incongruent cue-target combinations. Simulated ITs can be observed in Figure 5B. The UAM exhibits the same qualitative pattern as the empirical data (see below for model fit). We next assessed whether IT distributions would be similar to those of typical two-choice speeded button press tasks. Figure 5C shows the IT distribution of a representative participant from our empirical data set, displaying a typical, positively skewed distri-

bution. As can be seen in Figure 4D, the IT distribution for a representative simulated participant is also positively skewed.

Movement times and movement paths. The empirical MTs and MPs appear in Figures 5A and 5C. Empirical MTs displayed the same pattern as empirical ITs (see Figure 5A). For congruent cue-target combinations, high probability cues induced faster MTs than low probability cues. This pattern reversed for incongruent cue-target combinations. Consistently, incongruent cue-target combinations elicited more curved MPs toward the competing target compared with congruent cue-target combinations. Furthermore, high probability incongruent cue-target combination MPs displayed the strongest curvature. Our model captures the qualitative pattern displayed by both the MTs and MPs (see Figure 5B and 5D, respectively).

Model fit and robustness. The simulated ITs and MTs produced a very good fit ($R^2 = 0.997$). To investigate model robustness to parameter setting, Figure 6 shows average R^2 heatmaps for different parameter settings (average is across the third parameter). Note that R^2 is consistently high across the entire grid. Hence, our model is robust to parameter setting, showing that the good fit is not due to parameter fitting, but rather to the model architecture.

Fixed decision bound emergence and task difficulty. The dynamical interaction between the STN activity and the absolute difference between M1 units is shown in Figure 7. To avoid overload in the figure, we only plot activation of the task-required M1 units, but these approximate well the absolute difference between M1 units. Figure 7 shows the dynamical interaction for two congruent cue-target trials with different probabilities (operationalizing task difficulty: high probability = easy, low probability = difficult). High probability in favor of an action plan induces a steep increase in motor units (dark blue full line); hence the difference between motor units also increases fast. This induces a steep decrease in STN activation (dark blue dashed line). In contrast, a low probability in favor of an action plan induces a mild increase in motor units (light blue full line), hence a slower increase in difference between M1 units, and a slower decrease in STN activation (light blue dashed line). This explains the observation that distinct ITs are reached at a similar M1 activity level, also when varying difficulty level (Churchland et al., 2008; Schall & Bichot, 1998). In other words, adaptive information flow exhibits a fixed decision bound as an emergent property, consistent with neurophysiological findings (e.g., Twomey et al., 2015).

Simulation 3: Numerical Cognition

In the UAM, domain-specific cognitive processes (implemented as stimulus-response mappings) interact with domain-general decision making and motor processes. As a consequence, we can plug in the latter in any (domain-)specific task. With this in mind, we set out to apply our model to a very different domain, namely numerical cognition. In a number comparison task, Santens et al. (2011) instructed subjects to reach for a left (right) target when a number was smaller (larger) than five, or vice versa. The study investigated the numerical distance effect (e.g., Moyer & Landauer, 1967; Van Opstal & Verguts, 2011), meaning that ITs increase as distance between the compared number and the referent number increases. For instance, comparing one and five is typically faster than comparing four and five. Santens et al. (2011) found the empirical signature of the distance effect in ITs and
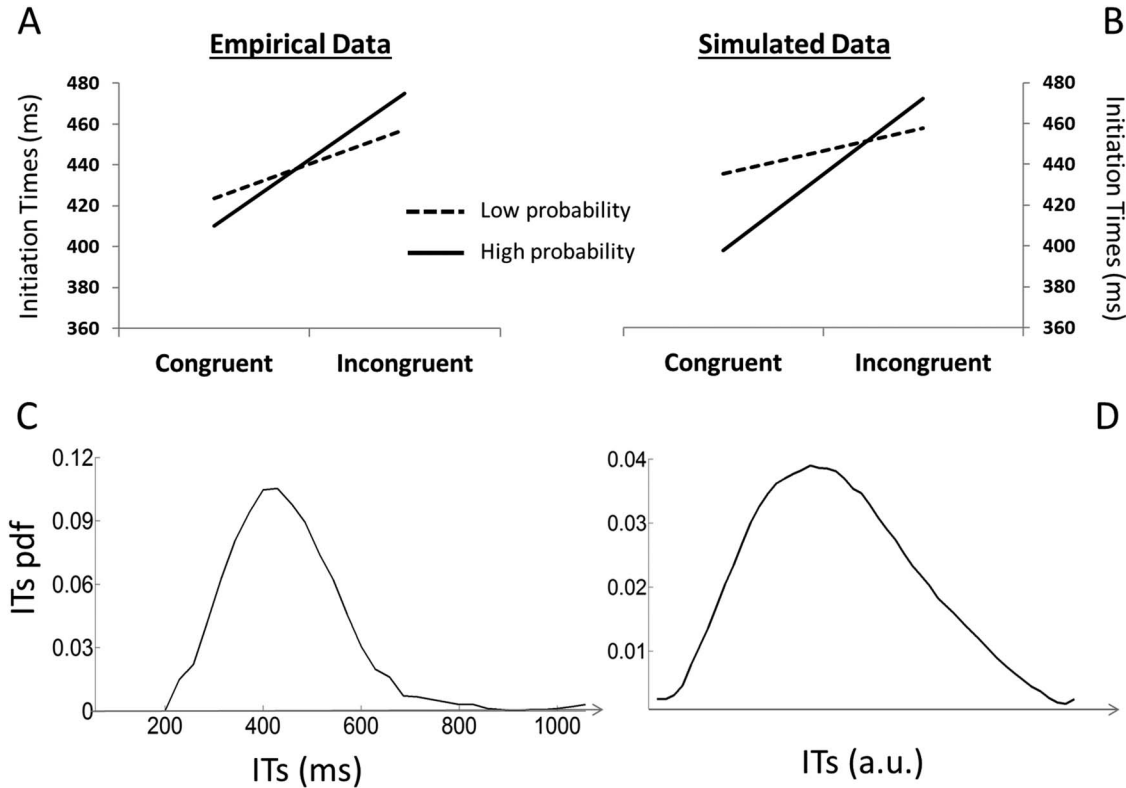
Figure 4. Simulation 2, Initiation Times. (A) Empirical data from Calderon et al. (2015). Graphical representation of the interaction between cue-target congruency and probability for ITs (i.e., the time interval between the go signal onset and leaving the start location square) in the experimental task. As can be observed, congruent trials are on average faster than incongruent trials. Moreover, for the congruent condition, high probable trials are faster than low probable trials, and this pattern reverses for the incongruent condition. (B) Similar for simulated ITs. (C) Initiation time probability density function (pdf) of a representative subject from Calderon et al. (2015). As can be observed, the IT pdf of this subject is again positively skewed ($\gamma = 0.79$). (D) IT for one representative simulated subject also exhibits a positively skewed distribution ($\gamma = 0.51$).

MTs. From the UAM point of view, however, comparison tasks are just another way to manipulate task difficulty. We thus tested whether our model could account for these data as well.

Method

Design. As in Santens et al. (2011), numbers one to nine (except five) were presented to the model, to be compared with five. Also as in Santens et al. (2011), the model reached as quickly as possible to a left-hand target if the number was smaller than five or to a right-hand target if it was larger than five (see Figure 8). ITs and MTs were computed as in Simulation 2; 4,000 trials were simulated with a similar trial distribution as in Santens et al. (2011).

Data analysis. Exactly the same τ, α, and STN values as in Simulation 2 were used. Input to PMd is shown in Appendix C (values similar to Van Opstal, Gevers, De Moor, & Verguts, 2008). As in Simulation 2, to evaluate model fit, the eight empirical ITs and MTs from Santens et al. (2011) were linearly regressed on the eight simulated ITs and MTs obtained from the model output.

Response implementation. Response implementation was identical to that of Simulation 2.

Results

The empirical results are illustrated in Figures 9A and 9C. The numerical distance effect is observed in the ITs (Figure 9A) and in the MTs (Figure 9C). Simulated ITs and MTs (again in arbitrary time units) appear in Figure 9B and 9D. As can be seen, our model exhibits the same qualitative pattern as the empirical data (also quantitatively the fit was excellent, $R^2 = 0.851$). Importantly, the parameters were not optimized for this specific task; instead, we took the exact same values as in Simulation 2. Still, again our model captures the distance effect in ITs and in MTs, demonstrating its robustness. Hence, it shows in a completely different domain the UAM's capacity to account for the influence of cognitive processes on movement execution.

General Discussion

We presented the unfolding action model (UAM) of continuous cognition-action interactions. The UAM core concept is to propose a third level to information processing flow. The model implements continuous information flow from the first to the last cognitive stage, but adaptive information flow between the last cognitive and motor
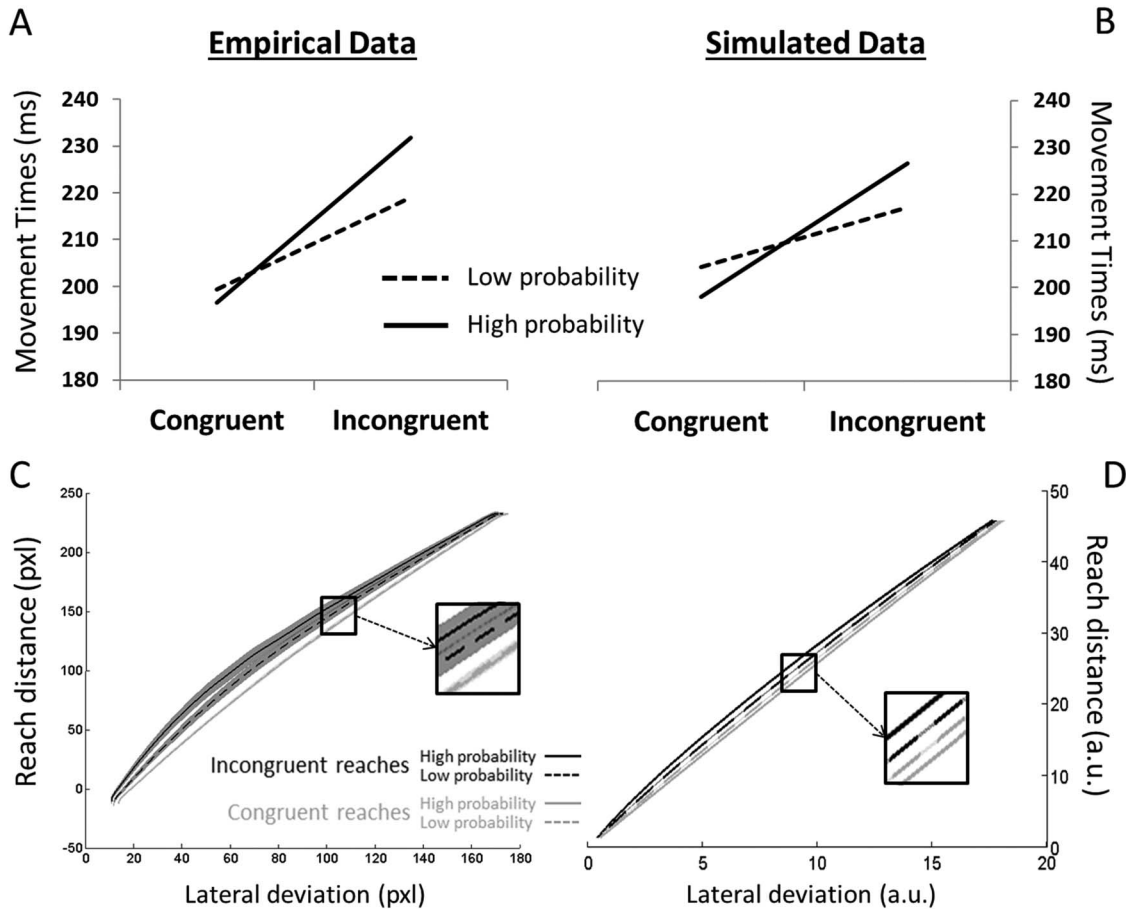
Figure 5. Simulation 2, Movement Times and Paths. (A) Average empirical movement times (Cue–Target Congruency × Probability Interaction). (B) Simulated movement times. (C) Same as A for empirical movement paths. Left reach trajectories were collapsed with right reach trajectories to simplify the figure. Congruent high and low-probability (plain and dashed gray) trajectories partly overlap in the figure. (D) Simulated movement paths. Shaded error bars in both movement path graphs represent the standard error of the mean.

stage. In the UAM, adaptive information flow is gated by the subthalamic nucleus (STN). In Simulation 1, we demonstrate that our model can account for empirical patterns of the classical 2AFC decision making task, namely positively skewed RT distributions and speed–accuracy trade-offs. In Simulation 2, we addressed MTs and MPs in a cognitive control task. We demonstrated that thresholded information flow emerges between cognition and action (i.e., fixed decision bound). In line with empirical data, we showed that both the initiation time and online movement were sensitive to cognitive factors such as task difficulty (implemented as prime-target congruity). Furthermore, we showed that motor activity reached the same threshold level prior to response initiation regardless of task difficulty. In Simulation 3, a completely different task was considered (number comparison task in numerical cognition). Without any parameter change, we demonstrated that the simulations again corresponded closely to empirical ITs and MTs.

Anatomical Simplifications

The input and motor layers did not receive an anatomical label, simply because it is not entirely clear which region exactly would

implement these functions. The input area may correspond to V1 and subsequent visual areas. The movement vector may be localized in either the spinal cord or the brainstem. Indeed, both are known to contain relatively high-order motor controllers (Swanson, 2012). Of course, the spine additionally contains motor neurons (directly controlling flexor and extensor muscles), but this level of detail is beyond the scope of the current model. Consequently, we lumped every neuron outside cortex or basal ganglia as belonging to "motor stage." Movement in the UAM derives from a spatial averaging of the relevant movement vectors. There is direct evidence for such spatial averaging in motor cortex (Georgopoulos, Schwartz, & Kettner, 1986; Suminski, Mardoum, Lillicrap, & Hatsopoulos, 2015). To our knowledge however, at the brainstem/spine level such averaging stands out for future research. Another simplification was the pathway from STN to motor cortex. Anatomically, STN excites globus pallidus pars interna and substantia nigra pars reticulata (SNr); these areas inhibit thalamus. In turn, thalamus excites motor cortex, closing the motor-basal ganglia loop (Redgrave et al., 2010). We also disregarded here the motor cortex basal ganglia direct and indirect
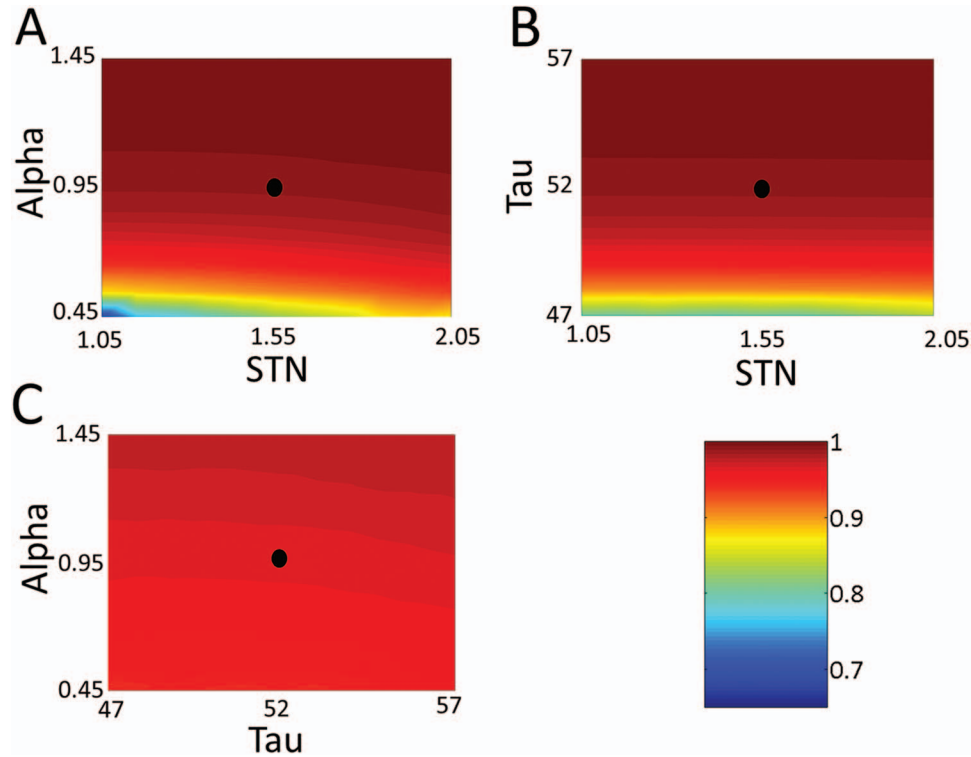
Figure 6. Simulation 2, Model Robustness. The three heat maps depict the mean R^2 value when varying two parameters and averaging across all the levels of the third parameter. In figure A, B and C we respectively vary STN/Alpha, STN/Tau, Tau/Alpha and average across Tau, Alpha and STN. The black dot represents the parameters value used to generate the simulated data. The color bar indicates the correlation coefficient for the three graphs. Note that the lowest value equals 0.65. See the online article for the color version of this figure.

pathways via striatum. Recent tractography and fMRI work suggest that the anatomical pathway from pre-SMA to striatum may partly control the response inhibition threshold and thus the what/when separation (Forstmann et al., 2008, 2010). Such anatomical simplifications allowed us to focus on the model functional properties, but future research should tighten the link with the anatomy.
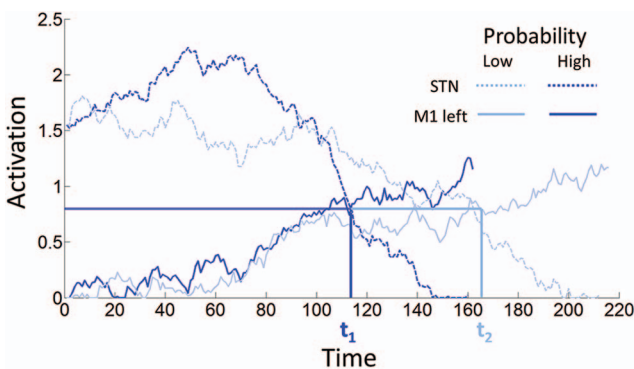

Figure 7. Simulation 2, Fixed Decision Bound Property Across Trials. We illustrate two congruent left reach trials. Line color saturation represents respectively a high (dark blue) and low (light blue) probability trial. Line styles depict the unit activation of M1 L (full line) and STN (dashed line). See the online article for the color version of this figure.

In the remainder of this article, we again revisit our core proposal, and while doing so discuss related models. Finally, we point to several avenues for future research.

Adaptive Information Flow

Our core proposal was to implement adaptive information flow between the last cognitive and motor stage. We here discuss some useful computational (what/when dissociation) and empirical (emergence of a fixed decision bound and temporal overlap between cognition and action) consequences of this concept. We also broaden it to other stages and discuss related proposals in the literature.

What/When Dissociation

Computational models of cognition typically do not separate what action to select from when to implement it. They implement behavioral execution as starting when motor activation crosses a fixed bound (e.g., Gold & Shadlen, 2007). Of course, it is possible to prolong a model's response time (and thus increase the "when to respond") by simply adding a fixed encoding or motor constant (e.g., as in the DDM; Ratcliff, 1978). Alternatively, one could increase the response threshold in order to delay the "when" to respond (Herz, Zavala, Bogacz, & Brown, 2016; Mansfield, Karayanidis, Jamadar, Heathcote, & Forstmann, 2011). However,
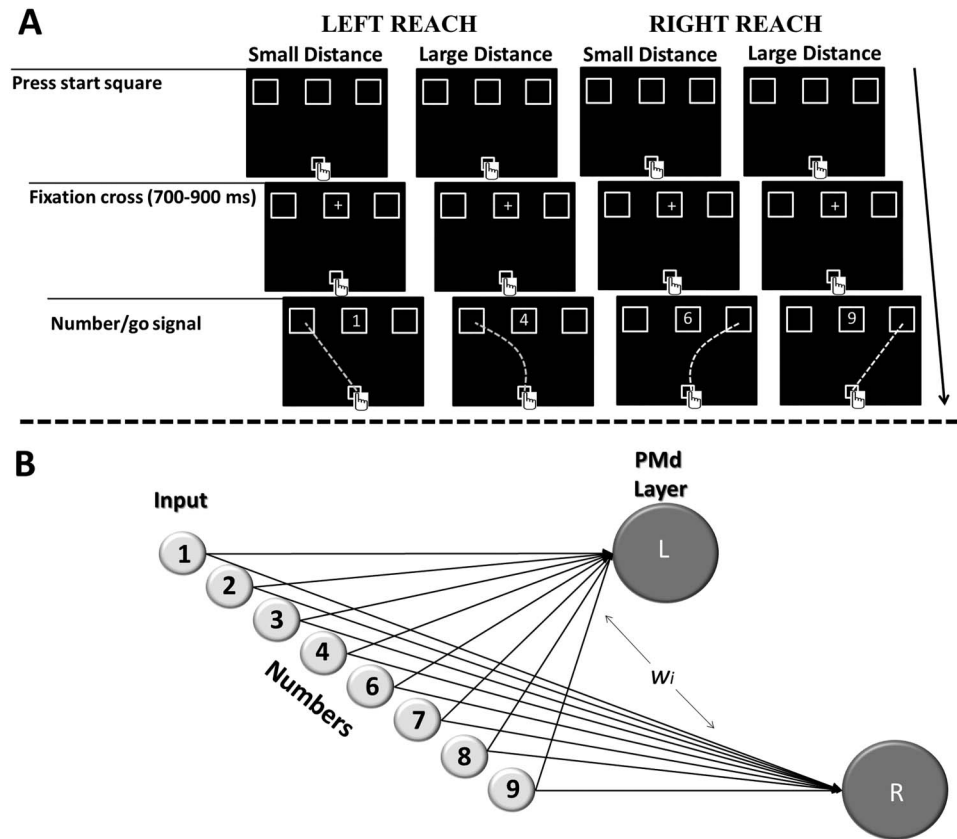
Figure 8. Simulation 3 Outline. (A) Experimental task design of Santens et al., (2011). Participants first pressed a start square at the bottom of the screen, triggering the presentation of a fixation cross in the upper central square. After a jittered amount of time, a number replaced the fixation cross and participants had to reach the left upper square when the number was smaller than five and the right upper square number when it was larger than five. (B) Mapping used in Simulation 3. Each stimulus is connected to the PMd layer unit with a certain weight (see Appendix C for input-PMd weight connection values).

such a parametric modulation does not elucidate how or why the cognitive system can optimally choose the timing of response execution.

In the UAM, a what/when dissociation was achieved by creating a negative feedback loop between M1 and STN. In particular, when the system is uncertain about what action to perform, it withholds responding. Related what/when dissociations have been proposed in the literature, such as the basal ganglia model developed by Frank (2006; also see Frank, Samanta, Moustafa, & Sherman, 2007). As in the UAM, the basal ganglia model dissociates what action to perform from when to execute it based on a negative feedback loop between (pre)motor cortex and STN. However, contrary to the UAM, the basal ganglia model does not implement adaptive information flow between the last cognitive stage and motor stage. Instead, it implements cognition-action thresholding. Therefore, the basal ganglia model cannot account for the influence of cognitive factors on overt movement execution.

We opted for response conflict as a convenient criterion for choosing when to withhold responding (as in Frank, 2006). In general, we envision that the STN may learn when to withhold responding depending on task and contextual constraints. In particular, by using reinforcement learning principles, the STN may learn when to gate responses into the motor stage, and thus to optimally "decide" when to allow action execution (O'Reilly & Frank, 2006). For example, consider again the cueing task of Simulation 2. When the proportion of incongruent trials is large, subjects tend to become more cautious. In the model, this could be implemented by strong excitatory weights from motor cortex to the STN, thus effectively letting subjects shift on the speed/accuracy continuum. By adaptively modifying the weights from M1 to STN, the UAM could learn what M1 activity pattern should modulate STN activity for optimal responding. Further note that any task, irrespective of its stimuli or even input modality, makes use of the same weights between M1 and STN. Therefore, the UAM predicts that response conservativeness obtained through learned M1-to-STN weights during a specific task, should generalize to tasks involving completely distinct stimuli. This remains to be tested.

Other models have suggested different mechanisms to address the what/when dissociation. For instance, a probabilistically motivated proposal appears in Bogacz and Gurney (2007). These authors propose that the STN computes the normalization constant required to calculate the probability that a specific response is valid. When several options are equally likely (active), each option becomes less likely to pass the threshold, and the normalization
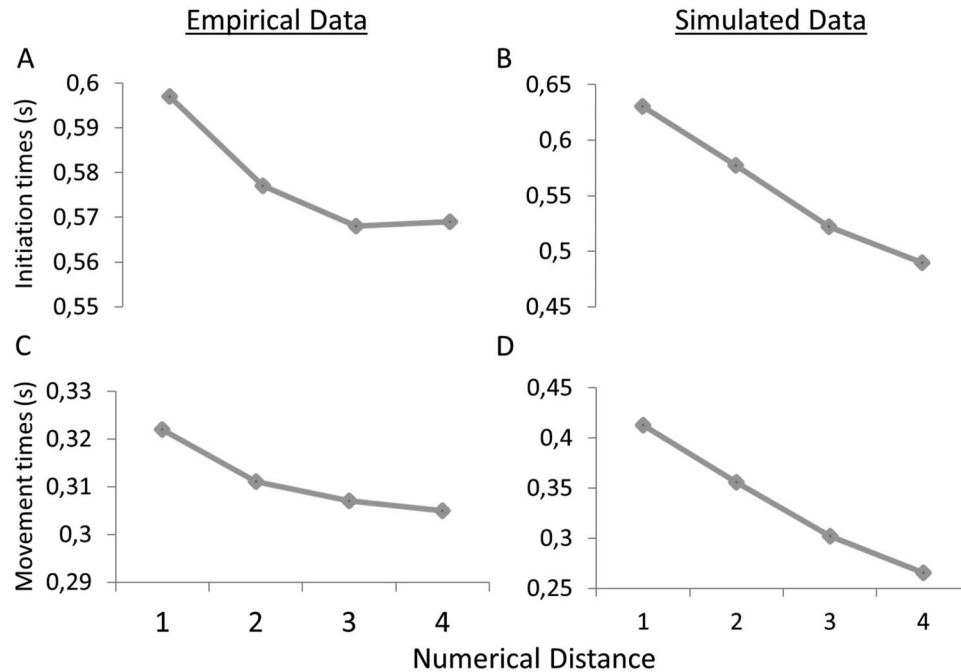
Empirical Data   **Simulated Data**

Figure 9. Simulation 3, Empirical Data From Santens et al. (2011) and Simulated Data. (A) The numerical distance effect for initiation times. (B) Simulated initiation times. (C) Same as A for the MTs (i.e., the time interval between leaving the start location square and entering the target location square). (D) Simulated MTs.

constant is large. This normalization constant can thus be thought of as representing response conflict (Botvinick et al., 2001), where a large (small) normalization constant is associated to high (low) response conflict. Thus, the normalization constant puts a dynamical brake on action initiation. Another model appeared in Niv, Daw, Joel, and Dayan (2007). These authors propose that there is a cost to fast action implementation; very fast action onsets would entail a larger execution cost. In a reinforcement learning framework, they suggest that both what behavior to choose and when to do it, are decided by optimizing a joint reward/cost function. Lastly, a recent alternative account proposes that what/when dissociations are achieved through a process of time-varying optimal decision bounds (Malhotra, Leslie, Ludwig, & Bogacz, 2017). Here, reaching or not reaching a decision bound is respectively reconceptualized as deciding to commit to a specific action or deciding instead to accumulate more evidence (i.e., wait before committing to an action). Malhotra, Leslie, Ludwig, and Bogacz (2017) suggest that committing or not to a specific action depends on the uncertainty regarding (the distribution of) trial difficulty.

Emergence of a Fixed Decision Threshold

As previously described, computational models typically implement cognition-action thresholding, that is, discrete step in the information flow between the last cognitive and motor stage. This implementation is also known as a fixed decision bound in accumulation-to-bound models (e.g., Forstmann, Ratcliff, & Wagenmakers, 2015; Ratcliff, 1978). However, these models do not explain how this bound emerges from the interplay between the dynamical activity of distinct brain regions. In the UAM, decision bounds are not fixed but emerge from the dependency

between motor cortices and STN activity, inducing an approximately linear decrease of the STN activity. This dependency approximates a fixed-bound model (see Figure 2C and 7).

Not all models assume a fixed decision bound. Another important class of models propose that the evidence integration rate may be modified as a function of the urgency context (Cisek et al., 2009; Standage, You, Wang, & Dorris, 2011; Thura, Beauregard-Racine, Fradet, & Cisek, 2012). These models suggest that time pressure for the execution of a motor plan is integrated as a factor in the decision-making process. As the urgency to respond increases, so would the buildup rate of motor activity. For instance, the urgency-gating model (Cisek et al., 2009; Thura et al., 2012) accounts for action selection situations where temporal constraints play a significant role. In the urgency gating model, the rate of activity buildup is defined by the urgency parameter (typically proportional to elapsed time; Cisek et al., 2009). Such an implementation can be reconceptualized as collapsing bounds to the decision process (for review see Hawkins, Forstmann, Wagenmakers, Ratcliff, & Brown, 2015). In principle, the UAM can also approximate a collapsing bound model by letting STN activity decrease nonlinearly. Such a nonlinear decrease would be very naturally implemented by having STN receive other signals that can be integrated alongside signals from motor cortex (e.g., urgency signals; van Maanen, Fontanesi, Hawkins, & Forstmann, 2016).

Temporal Overlap Between Cognitive and Motor Processes

By implementing adaptive information flow between the last cognitive and motor stage, an emergent property of the UAM appears, namely that cognitive effects leak into action. Any model

implementing cognition-action thresholding is unable to account for any influence of cognitive factors on movement execution. This is not problematic when accounting for discrete behavioral measures such a button presses. Indeed, button presses tend to hide the continuous effects of cognition on action. However, the advent of reaching task studies (Song & Nakayama, 2009) force scientists to develop models that can account for the typical behavioral patterns in button press studies, and simultaneously explain how cognitive factors influence overt execution. In the UAM, we show that adaptive information flow can bridge the gap between traditional button press models (Ratcliff, 1978) and novel data showing a continuous interaction between cognitive and motor processes (Calderon et al., 2017). Finally, one might wonder what is adaptive about letting cognition "leak" into action, outside of providing cognitive scientists another dependent variable to model. We propose that this leak is a consequence of the what/when dissociation that the brain must implement for adaptive decision making.

Neurally and behaviorally, due both to individual differences and noise at different processing stages, task performance sometimes may seem to either stem from overlapping or nonoverlapping cognitive and motor processes. Adaptive information flow can mimic both cases. Indeed, the system can potentially learn, by setting appropriate weights of the M1-STN projections, to behave within a continuum of fully overlapping (i.e., continuous information flow) or fully discrete (i.e., thresholded information flow) cognitive and motor processes. Take the case of an individual who shows little or no effect of cognitive factors on their overt movement execution. In the UAM, this would be accounted for by small M1-STN weights. Indeed, with small weights, the difference between competing M1 units will need to be large (i.e., conflict will be fully [or close to] resolved) for movement initiation to start. In turn, the effects of cognitive factors will influence the time it takes to initiate a movement rather than the movement itself (i.e., cognition will not leak into action). In contrast, envisage an individual showing a strong effect of cognitive factors on their actions. In this case, the UAM would account for such behavior by having large M1-STN weights. With large weights, the difference between competing M1 units will be small (i.e., conflict will not be resolved) when movement initiation starts. Hence, the effects of cognitive factors will not only have an influence on the time needed to initiate a movement but also on the movement itself (i.e., cognition will leak into action).

Output Gating

Theoretically, adaptive information flow can be implemented at distinct stages of information processing. Indeed, negative feedback loops can be implemented between distinct regions of the brain (i.e., processing stages) and basal ganglia nuclei (such as the STN). This proposal is called output gating (Chatham, Frank, & Badre, 2014; Hochreiter & Schmidhuber, 1997; Kriete, Noelle, Cohen, & O'Reilly, 2013). Output gating refers to holding information in working memory until the appropriate time for letting it go to subsequent stages has arrived. This is the same what/when dissociation as we discussed for the cognitive to motor gap, but applied to cognitive actions like "keeping information in working memory." Output gating models propose that learning when to gate information out of working memory is a separate subtask to be learned, obeying the same reinforcement learning principles as

the overt task of learning what button to press. In such a system we can set, for each contiguous pair of stages, and even on a trial-by-trial basis, information flow on a continuum between continuous and thresholded. Thereby, one can imagine a system that has, for example, continuous information flow between Stages 1 and 2, but thresholded information flow between Stages 2 and 3. As already mentioned, future UAM work is planned to make the output gate dependent on reinforcement-based feedback.

Relation to Dynamic Field Theory

We considered just two points in the movement space for each task, each corresponding to a specific movement direction (movement vector). This was done because it allowed us to merge cognitive movement data (Simulations 1–3) more easily with the biology of movement and inhibition. Future work should extend our framework toward more continuous movements (Christopoulos, Bonaiuto, & Andersen, 2015). This extension can be implemented by using dynamic neural fields (Cisek, 2006; Klaes, Schneegans, Schöner, & Gail, 2012). Here, movement is considered as a point in a multidimensional space, where each dimension represents a movement characteristic such as direction, speed, or vigor. Movement is constrained by activation from motor, memory, and cognitive layers (Erlhagen & Schöner, 2002; Schöner & Thelen, 2006). These neural fields describe the activation distributions over the movement vector feature space (e.g., Erlhagen, Bastian, Jancke, Riehle, & Schöner, 1999). Such a move would allow us to extend our model and account for more naturalistic reaches in a three-dimensional space (e.g., Chapman et al., 2010; Gallivan & Chapman, 2014).

Broadening the UAM Task Scope

The current model allows consideration of many more tasks and contexts than just those reported here. A first example would be the go/no-go task (Gomez, Ratcliff, & Perea, 2007). As just mentioned, in the applications considered up to now, movement resulted from two fixed vectors (pointing left and right, respectively). However, in the context of the go/no-go task, it is straightforward to envisage that the STN itself competes against movement toward a specific button. Indeed, a strongly supported possibility is that the right inferior frontal cortex feeds a response inhibition signal to the STN, thereby biasing the competition in favor of the STN (for review see Aron, Robbins, & Poldrack, 2014). Hence, this response inhibition would make sure that the adaptive information flow gate remains closed and action is withheld.

A second task, namely the stop-signal task (Logan, Cowan, & Davis, 1984), could be modeled in a very similar fashion. This task has been modeled extensively as an independent race between one or more responses and the stop response (e.g., Boucher, Palmeri, Logan, & Schall, 2007; Logan, Van Zandt, Verbruggen, & Wagenmakers, 2014). In the current framework, a stop task would be implemented by adding another excitatory input to the STN (for instance from striatal no-go neurons, see Collins & Frank, 2013). This input would activate STN and thus exhibit an opposite effect as M1 units. In turn STN activation would maintain the adaptive information flow gate closed. In line with this view, recent work suggests that successful motor inhibition results from stop-cue

related information being transmitted from the striatum, through the globus pallidus, to the STN (Schmidt, Leventhal, Mallet, Chen, & Berke, 2013).

Third, a natural application for our model is the "reach/point to X" task, where movement paths can be measured (e.g., Sullivan et al., 2015). An instance of this paradigm is the "point to number" task (Dotan & Dehaene, 2016; Siegler & Opfer, 2003), where a subject is required to point on a physical line to where the corresponding number would be situated on a number line. By modeling movement time and paths, in addition to response time to choices, our model can address "reach/point to X" tasks that investigate the temporal dynamics of action selection processes (Boulenger et al., 2006; Cressman et al., 2007; McKinstry, Dale, & Spivey, 2008; Resulaj et al., 2009; Spivey et al., 2005).

Conclusion

We proposed a neurocomputational model based on the theoretical framework of integrative information processing suggesting a parallel implementation of perceptual, cognitive, and motor processes (Cisek, 2007; Friston, 2010; Gibson, 1979). Modeling behavior as a continuous cognition-action interaction refereed by the dynamic interplay between the basal ganglia (McHaffie, Stanford, Stein, Coizet, & Redgrave, 2005), in particular the STN (Frank, 2006), and sensorimotor cortices (Cisek & Kalaska, 2010), accounts for many empirical effects of cognition on action initiation and execution (Calderon et al., 2015). It also explains ubiquitous behavioral and neurophysiological patterns (i.e., positive skew, speed–accuracy trade-off, emergence of a fixed decision threshold). Perhaps more importantly, the model opens doors for future research on interactions between neurophysiology, cognition, and action dynamics.

References

Alexander, G. E., & Crutcher, M. D. (1990). Functional architecture of basal ganglia circuits: Neural substrates of parallel processing. *Trends in Neurosciences, 13,* 266–271. http://dx.doi.org/10.1016/0166-2236(90)90107-L

Aron, A. R., Durston, S., Eagle, D. M., Logan, G. D., Stinear, C. M., & Stuphorn, V. (2007). Converging evidence for a fronto-basal-ganglia network for inhibitory control of action and cognition. *Journal of Neuroscience, 27,* 11860–11864.

Aron, A. R., & Poldrack, R. A. (2006). Cortical and subcortical contributions to Stop signal response inhibition: Role of the subthalamic nucleus. *The Journal of Neuroscience, 26,* 2424–2433. http://dx.doi.org/10.1523/JNEUROSCI.4682-05.2006

Aron, A. R., Robbins, T. W., & Poldrack, R. A. (2014). Inhibition and the right inferior frontal cortex: One decade on. *Trends in Cognitive Sciences, 18,* 177–185. http://dx.doi.org/10.1016/j.tics.2013.12.003

Atkinson, R. C., Holmgren, J., & Juola, J. F. (1969). Processing time as influenced by the number of elements in a visual display. *Attention, Perception & Psychophysics, 6,* 321–326. http://dx.doi.org/10.3758/BF03212784

Bastian, A., Schöner, G., & Riehle, A. (2003). Preshaping and continuous evolution of motor cortical representations during movement preparation. *The European Journal of Neuroscience, 18,* 2047–2058. http://dx.doi.org/10.1046/j.1460-9568.2003.02906.x

Baunez, C., Humby, T., Eagle, D. M., Ryan, L. J., Dunnett, S. B., & Robbins, T. W. (2001). Effects of STN lesions on simple vs choice reaction time tasks in the rat: Preserved motor readiness, but impaired response selection. *The European Journal of Neuroscience, 13,* 1609–1616. http://dx.doi.org/10.1046/j.0953-816x.2001.01521.x

Baunez, C., & Robbins, T. W. (1997). Bilateral lesions of the subthalamic nucleus induce multiple deficits in an attentional task in rats. *The European Journal of Neuroscience, 9,* 2086–2099. http://dx.doi.org/10.1111/j.1460-9568.1997.tb01376.x

Bogacz, R., & Gurney, K. (2007). The basal ganglia and cortex implement optimal decision making between alternative actions. *Neural Computation, 19,* 442–477. http://dx.doi.org/10.1162/neco.2007.19.2.442

Bogacz, R., Wagenmakers, E.-J., Forstmann, B. U., & Nieuwenhuis, S. (2010). The neural basis of the speed-accuracy tradeoff. *Trends in Neurosciences, 33,* 10–16. http://dx.doi.org/10.1016/j.tins.2009.09.002

Botvinick, M. M., Braver, T. S., Barch, D. M., Carter, C. S., & Cohen, J. D. (2001). Conflict monitoring and cognitive control. *Psychological Review, 108,* 624–652. http://dx.doi.org/10.1037/0033-295X.108.3.624

Boucher, L., Palmeri, T. J., Logan, G. D., & Schall, J. D. (2007). Inhibitory control in mind and brain: An interactive race model of countermanding saccades. *Psychological Review, 114,* 376–397. http://dx.doi.org/10.1037/0033-295X.114.2.376

Boulenger, V., Roy, A. C., Paulignan, Y., Deprez, V., Jeannerod, M., & Nazir, T. A. (2006). Cross-talk between language processes and overt motor behavior in the first 200 msec of processing. *Journal of Cognitive Neuroscience, 18,* 1607–1615. http://dx.doi.org/10.1162/jocn.2006.18.10.1607

Boy, F., Husain, M., & Sumner, P. (2010). Unconscious inhibition separates two forms of cognitive control. *Proceedings of the National Academy of Sciences of the United States of America, 107,* 11134–11139. http://dx.doi.org/10.1073/pnas.1001925107

Calderon, B. C., Dewulf, M., Gevers, W., & Verguts, T. (2017). Continuous track paths reveal additive evidence integration in multistep decision making. *Proceedings of the National Academy of Sciences of the United States of America, 114,* 10618–10623. http://dx.doi.org/10.1073/pnas.1710913114

Calderon, C. B., Verguts, T., & Gevers, W. (2015). Losing the boundary: Cognition biases action well after action selection. *Journal of Experimental Psychology: General, 144,* 737–743. http://dx.doi.org/10.1037/xge0000087

Capaldi, E. J., & Miller, D. J. (1988). Counting in rats: Its functional significance and the independent cognitive processes that constitute it. *Journal of Experimental Psychology: Animal Behavior Processes, 14,* 3–17. http://dx.doi.org/10.1037/0097-7403.14.1.3

Cavanagh, J. F., Wiecki, T. V., Cohen, M. X., Figueroa, C. M., Samanta, J., Sherman, S. J., & Frank, M. J. (2011). Subthalamic nucleus stimulation reverses mediofrontal influence over decision threshold. *Nature Neuroscience, 14,* 1462–1467. http://dx.doi.org/10.1038/nn.2925

Chapman, C. S., Gallivan, J. P., Wood, D. K., Milne, J. L., Culham, J. C., & Goodale, M. A. (2010). Reaching for the unknown: Multiple target encoding and real-time decision-making in a rapid reach task. *Cognition, 116,* 168–176. http://dx.doi.org/10.1016/j.cognition.2010.04.008

Chatham, C. H., Frank, M. J., & Badre, D. (2014). Corticostriatal output gating during selection from working memory. *Neuron, 81,* 930–942. http://dx.doi.org/10.1016/j.neuron.2014.01.002

Christopoulos, V., Bonaiuto, J., & Andersen, R. A. (2015). A biologically plausible computational theory for value integration and action selection in decisions with competing alternatives. *PLoS Computational Biology, 11,* e1004104. http://dx.doi.org/10.1371/journal.pcbi.1004104

Churchland, A. K., Kiani, R., & Shadlen, M. N. (2008). Decision-making with multiple alternatives. *Nature Neuroscience, 11,* 693–702. http://dx.doi.org/10.1038/nn.2123

Cisek, P. (2006). Integrated neural processes for defining potential actions and deciding between them: A computational model. *The Journal of Neuroscience, 26,* 9761–9770. http://dx.doi.org/10.1523/JNEUROSCI.5605-05.2006

Cisek, P. (2007). Cortical mechanisms of action selection: The affordance competition hypothesis. *Philosophical Transactions of the Royal Society of London Series B, Biological Sciences, 362,* 1585–1599. http://dx.doi.org/10.1098/rstb.2007.2054

Cisek, P., & Kalaska, J. F. (2005). Neural correlates of reaching decisions in dorsal premotor cortex: Specification of multiple direction choices and final selection of action. *Neuron, 45,* 801–814. http://dx.doi.org/10.1016/j.neuron.2005.01.027

Cisek, P., & Kalaska, J. F. (2010). Neural mechanisms for interacting with a world full of action choices. *Annual Review of Neuroscience, 33,* 269–298. http://dx.doi.org/10.1146/annurev.neuro.051508.135409

Cisek, P., Puskas, G. A., & El-Murr, S. (2009). Decisions in changing conditions: The urgency-gating model. *The Journal of Neuroscience, 29,* 11560–11571. http://dx.doi.org/10.1523/JNEUROSCI.1844-09.2009

Collins, A. G. E., & Frank, M. J. (2013). Cognitive control over learning: Creating, clustering, and generalizing task-set structure. *Psychological Review, 120,* 190–229. http://dx.doi.org/10.1037/a0030852

Collins, A. M., & Loftus, E. F. (1975). A Spreading-Activation Theory of Semantic Processing. *Psychological Review, 82,* 407–428. http://dx.doi.org/10.1037/0033-295X.82.6.407

Cressman, E. K., Franks, I. M., Enns, J. T., & Chua, R. (2007). On-line control of pointing is modified by unseen visual shapes. *Consciousness and Cognition, 16,* 265–275. http://dx.doi.org/10.1016/j.concog.2006.06.003

Daw, N. D., Niv, Y., & Dayan, P. (2005). Uncertainty-based competition between prefrontal and dorsolateral striatal systems for behavioral control. *Nature Neuroscience, 8,* 1704–1711. http://dx.doi.org/10.1038/nn1560

Di Lazzaro, V., Oliviero, A., Profice, P., Insola, A., Mazzone, P., Tonali, P., & Rothwell, J. C. (1999). Direct demonstration of interhemispheric inhibition of the human motor cortex produced by transcranial magnetic stimulation. *Experimental Brain Research, 124,* 520–524. http://dx.doi.org/10.1007/s002210050648

Donders, F. C. (1868). Over de snelheid van psychische processen [On the speed of mental processes]. *Onderzoekingen gedaan in het Physiologisch Laboratorium der Utrechtsche Hoogeschool (1868–1869), 2,* 92–120.

Donders, F. C. (1969). On the speed of mental processes. *Acta Psychologica, 30,* 412–431. http://dx.doi.org/10.1016/0001-6918(69)90065-1

Donner, T. H., Siegel, M., Fries, P., & Engel, A. K. (2009). Buildup of choice-predictive activity in human motor cortex during perceptual decision making. *Current Biology, 19,* 1581–1585. http://dx.doi.org/10.1016/j.cub.2009.07.066

Dotan, D., & Dehaene, S. (2016). On the origins of logarithmic number-to-position mapping. *Psychological Review, 123,* 637–666. http://dx.doi.org/10.1037/rev0000038

Dum, R. P., & Strick, P. L. (2002). Motor areas in the frontal lobe of the primate. *Physiology & Behavior, 77,* 677–682. http://dx.doi.org/10.1016/S0031-9384(02)00929-0

Duque, J., Murase, N., Celnik, P., Hummel, F., Harris-Love, M., Mazzocchio, R., . . . Cohen, L. G. (2007). Intermanual differences in movement-related interhemispheric inhibition. *Journal of Cognitive Neuroscience, 19,* 204–213. http://dx.doi.org/10.1162/jocn.2007.19.2.204

Eriksen, C. W., & Schultz, D. W. (1979). Information processing in visual search: A continuous flow conception and experimental results. *Perception & Psychophysics, 25,* 249–263. http://dx.doi.org/10.3758/BF03198804

Erlhagen, W., Bastian, A., Jancke, D., Riehle, A., & Schöner, G. (1999). The distribution of neuronal population activation (DPA) as a tool to study interaction and integration in cortical representations. *Journal of Neuroscience Methods, 94,* 53–66. http://dx.doi.org/10.1016/S0165-0270(99)00125-9

Erlhagen, W., & Schöner, G. (2002). Dynamic field theory of movement preparation. *Psychological Review, 109,* 545–572. http://dx.doi.org/10.1037/0033-295X.109.3.545

Ferbert, A., Priori, A., Rothwell, J. C., Day, B. L., Colebatch, J. G., & Marsden, C. D. (1992). Interhemispheric inhibition of the human motor cortex. *The Journal of Physiology, 453,* 525–546. http://dx.doi.org/10.1113/jphysiol.1992.sp019243

Fleming, S. M., & Daw, N. D. (2017). Self-evaluation of decision-making: A general Bayesian framework for metacognitive computation. *Psychological Review, 124,* 91–114. http://dx.doi.org/10.1037/rev0000045

Fodor, J. A. (1983). *Modularity of mind.* Cambridge, MA: MIT Press.

Forstmann, B. U., Anwander, A., Schäfer, A., Neumann, J., Brown, S., Wagenmakers, E.-J., . . . Turner, R. (2010). Cortico-striatal connections predict control over speed and accuracy in perceptual decision making. *Proceedings of the National Academy of Sciences of the United States of America, 107,* 15916–15920. http://dx.doi.org/10.1073/pnas.1004932107

Forstmann, B. U., Dutilh, G., Brown, S., Neumann, J., von Cramon, D. Y., Ridderinkhof, K. R., & Wagenmakers, E.-J. (2008). Striatum and pre-SMA facilitate decision-making under time pressure. *Proceedings of the National Academy of Sciences of the United States of America, 105,* 17538–17542. http://dx.doi.org/10.1073/pnas.0805903105

Forstmann, B. U., Ratcliff, R., & Wagenmakers, E.-J. (2015). Sequential sampling models in cognitive neuroscience: Advantages, applications, and extensions. *Annual Review of Psychology, 67,* 641–666.

Frank, M. J. (2006). Hold your horses: A dynamic computational role for the subthalamic nucleus in decision making. *Neural Networks, 19,* 1120–1136. http://dx.doi.org/10.1016/j.neunet.2006.03.006

Frank, M. J., Samanta, J., Moustafa, A. A., & Sherman, S. J. (2007). Hold your horses: Impulsivity, deep brain stimulation, and medication in parkinsonism. *Science, 318,* 1309–1312. http://dx.doi.org/10.1126/science.1146157

Friston, K. (2010). The free-energy principle: A unified brain theory? *Nature Reviews Neuroscience, 11,* 127–138. http://dx.doi.org/10.1038/nrn2787

Gallivan, J. P., & Chapman, C. S. (2014). Three-dimensional reach trajectories as a probe of real-time decision-making between multiple competing targets. *Frontiers in Neuroscience, 8,* 215.

Georgopoulos, A. P., Schwartz, A. B., & Kettner, R. E. (1986). Neuronal population coding of movement direction. *Science, 233,* 1416–1419. http://dx.doi.org/10.1126/science.3749885

Gevers, W., Verguts, T., Reynvoet, B., Caessens, B., & Fias, W. (2006). Numbers and space: A computational model of the SNARC effect. *Journal of Experimental Psychology: Human Perception and Performance, 32,* 32–44. http://dx.doi.org/10.1037/0096-1523.32.1.32

Gibson, J. J. (1979). *The ecological approach to visual perception.* Boston, MA: Houghton.

Gilbert, S. J., & Shallice, T. (2002). Task switching: A PDP model. *Cognitive Psychology, 44,* 297–337. http://dx.doi.org/10.1006/cogp.2001.0770

Gold, J. I., & Shadlen, M. N. (2007). The neural basis of decision making. *Annual Review of Neuroscience, 30,* 535–574. http://dx.doi.org/10.1146/annurev.neuro.29.051605.113038

Gomez, P., Ratcliff, R., & Perea, M. (2007). A model of the go/no-go task. *Journal of Experimental Psychology: General, 136,* 389–413. http://dx.doi.org/10.1037/0096-3445.136.3.389

Gough, P. B. (1972). One second of reading. *Visible Language, 6,* 291–320.

Hawkins, G. E., Forstmann, B. U., Wagenmakers, E. J., Ratcliff, R., & Brown, S. D. (2015). Revisiting the evidence for collapsing boundaries and urgency signals in perceptual decision-making. *The Journal of Neuroscience, 35,* 2476–2484. http://dx.doi.org/10.1523/JNEUROSCI.2410-14.2015

Heitz, R. P. (2014). The speed-accuracy tradeoff: History, physiology, methodology, and behavior. *Frontiers in Neuroscience, 8,* 1–19. http://dx.doi.org/10.3389/fnins.2014.00150

Herz, D. M., Zavala, B. A., Bogacz, R., & Brown, P. (2016). Neural correlates of decision thresholds in the human subthalamic nucleus. *Current Biology, 26,* 916–920. http://dx.doi.org/10.1016/j.cub.2016.01.051

Hochreiter, S., & Schmidhuber, J. (1997). Long short-term memory. *Neural Computation, 9,* 1735–1780. http://dx.doi.org/10.1162/neco.1997.9.8.1735

Jahanshahi, M., Ardouin, C. M., Brown, R. G., Rothwell, J. C., Obeso, J., Albanese, A., . . . Limousin-Dowsey, P. (2000). The impact of deep brain stimulation on executive function in Parkinson's disease. *Brain, 123,* 1142–1154. http://dx.doi.org/10.1093/brain/123.6.1142

Keele, S. W. (1968). Movement control in skilled motor performance. *Psychological Bulletin, 70,* 387–403. http://dx.doi.org/10.1037/h0026739

Klaes, C., Schneegans, S., Schöner, G., & Gail, A. (2012). Sensorimotor learning biases choice behavior: A learning neural field model for decision making. *PLoS Computational Biology, 8,* e1002774. http://dx.doi.org/10.1371/journal.pcbi.1002774

Klaes, C., Westendorff, S., Chakrabarti, S., & Gail, A. (2011). Choosing goals, not rules: Deciding among rule-based action plans. *Neuron, 70,* 536–548. http://dx.doi.org/10.1016/j.neuron.2011.02.053

Kriete, T., Noelle, D. C., Cohen, J. D., & O'Reilly, R. C. (2013). Indirection and symbol-like processing in the prefrontal cortex and basal ganglia. *Proceedings of the National Academy of Sciences of the United States of America, 110,* 16390–16395. http://dx.doi.org/10.1073/pnas.1303547110

Lauwereyns, J., Watanabe, K., Coe, B., & Hikosaka, O. (2002). A neural correlate of response bias in monkey caudate nucleus. *Nature, 418,* 413–417. http://dx.doi.org/10.1038/nature00892

Logan, G. D., Cowan, W. B., & Davis, K. A. (1984). On the ability to inhibit simple and choice reaction time responses: A model and a method. *Journal of Experimental Psychology: Human Perception and Performance, 10,* 276–291. http://dx.doi.org/10.1037/0096-1523.10.2.276

Logan, G. D., Van Zandt, T., Verbruggen, F., & Wagenmakers, E.-J. (2014). On the ability to inhibit thought and action: General and special theories of an act of control. *Psychological Review, 121,* 66–95. http://dx.doi.org/10.1037/a0035230

Luce, R. D. (1986). *Response times: Their role in inferring elementary mental organization.* New York, NY: Oxford University Press.

Luppino, G., & Rizzolatti, G. (2000). The organization of the frontal motor cortex. *News in Physiological Sciences, 15,* 219–224. Retrieved from http://www.ncbi.nlm.nih.gov/pubmed/11390914

Magnuson, J. S. (2005). Moving hand reveals dynamics of thought. *Proceedings of the National Academy of Sciences of the United States of America, 102,* 9995–9996. http://dx.doi.org/10.1073/pnas.0504413102

Malhotra, G., Leslie, D. S., Ludwig, C. J. H., & Bogacz, R. (2017). Time-varying decision boundaries: Insights from optimality analysis. *Psychonomic Bulletin & Review.* Advance online publication. http://dx.doi.org/10.3758/s13423-017-1340-6

Mansfield, E. L., Karayanidis, F., Jamadar, S., Heathcote, A., & Forstmann, B. U. (2011). Adjustments of response threshold during task switching: A model-based functional magnetic resonance imaging study. *The Journal of Neuroscience, 31,* 14688–14692. http://dx.doi.org/10.1523/JNEUROSCI.2390-11.2011

Marconi, B., Genovesio, A., Giannetti, S., Molinari, M., & Caminiti, R. (2003). Callosal connections of dorso-lateral premotor cortex. *The European Journal of Neuroscience, 18,* 775–788. http://dx.doi.org/10.1046/j.1460-9568.2003.02807.x

Marr, D. (1976). Early processing of visual information. *Philosophical Transactions of the Royal Society of London, Series B, Biological Sciences, 275,* 483–519. http://dx.doi.org/10.1098/rstb.1976.0090

McClelland, J. L. (1979). On the time relations of mental processes: An examination of systems of processes in cascade. *Psychological Review, 86,* 287–330. http://dx.doi.org/10.1037/0033-295X.86.4.287

McCusker, L. X., Gough, P. B., & Bias, R. G. (1981). Word recognition inside out and outside in. *Journal of Experimental Psychology: Human Perception and Performance, 7,* 538–551. http://dx.doi.org/10.1037/0096-1523.7.3.538

McHaffie, J. G., Stanford, T. R., Stein, B. E., Coizet, V., & Redgrave, P. (2005). Subcortical loops through the basal ganglia. *Trends in Neurosciences, 28,* 401–407. http://dx.doi.org/10.1016/j.tins.2005.06.006

McKinstry, C., Dale, R., & Spivey, M. J. (2008). Action dynamics reveal parallel competition in decision making. *Psychological Science, 19,* 22–24. http://dx.doi.org/10.1111/j.1467-9280.2008.02041.x

Meyer, D. E., & Schvaneveldt, R. W. (1971). Facilitation in recognizing pairs of words: Evidence of a dependence between retrieval operations. *Journal of Experimental Psychology, 90,* 227–234. http://dx.doi.org/10.1037/h0031564

Michelet, T., Duncan, G. H., & Cisek, P. (2010). Response competition in the primary motor cortex: Corticospinal excitability reflects response replacement during simple decisions. *Journal of Neurophysiology, 104,* 119–127. http://dx.doi.org/10.1152/jn.00819.2009

Miller, G. A., Galanter, E., & Pribram, K. H. (1960). *Plans and the structure of behavior.* New York, NY: Henry Holt and Co, Inc. http://dx.doi.org/10.1037/10039-000

Mochizuki, H., Huang, Y.-Z., & Rothwell, J. C. (2004). Interhemispheric interaction between human dorsal premotor and contralateral primary motor cortex. *The Journal of Physiology, 561,* 331–338. http://dx.doi.org/10.1113/jphysiol.2004.072843

Mochizuki, H., Terao, Y., Okabe, S., Furubayashi, T., Arai, N., Iwata, N. K., . . . Ugawa, Y. (2004). Effects of motor cortical stimulation on the excitability of contralateral motor and sensory cortices. *Experimental Brain Research, 158,* 519–526. http://dx.doi.org/10.1007/s00221-004-1923-0

Moyer, R. S., & Landauer, T. K. (1967). Time required for judgements of numerical inequality. *Nature, 215,* 1519–1520. http://dx.doi.org/10.1038/2151519a0

Murphy, P. R., Robertson, I. H., Harty, S., & O'Connell, R. G. (2015). Neural evidence accumulation persists after choice to inform metacognitive judgments. *eLife, 4,* 1–23. http://dx.doi.org/10.7554/eLife.11946

Niv, Y., Daw, N. D., Joel, D., & Dayan, P. (2007). Tonic dopamine: Opportunity costs and the control of response vigor. *Psychopharmacology, 191,* 507–520. http://dx.doi.org/10.1007/s00213-006-0502-4

Oberauer, K., Souza, A. S., Druey, M. D., & Gade, M. (2013). Analogous mechanisms of selection and updating in declarative and procedural working memory: Experiments and a computational model. *Cognitive Psychology, 66,* 157–211. http://dx.doi.org/10.1016/j.cogpsych.2012.11.001

O'Connell, R. G., Dockree, P. M., & Kelly, S. P. (2012). A supramodal accumulation-to-bound signal that determines perceptual decisions in humans. *Nature Neuroscience, 15,* 1729–1735. http://dx.doi.org/10.1038/nn.3248

O'Reilly, R. C., & Frank, M. J. (2006). Making working memory work: A computational model of learning in the prefrontal cortex and basal ganglia. *Neural Computation, 18,* 283–328. http://dx.doi.org/10.1162/089976606775093909

Quillian, M. R. (1967). Word concepts: A theory and simulation of some basic semantic capabilities. *Behavioral Science, 12,* 410–430. http://dx.doi.org/10.1002/bs.3830120511

Quillian, M. R. (1969). The teachable language comprehender: A simulation program and theory of language. *Communications of the ACM, 12,* 459–476. http://dx.doi.org/10.1145/363196.363214

Ralph, M. A. L., Jefferies, E., Patterson, K., & Rogers, T. T. (2017). The neural and computational bases of semantic cognition. *Nature Reviews Neuroscience, 18,* 42–55. http://dx.doi.org/10.1038/nrn.2016.150

Ratcliff, R. (1978). A theory of memory retrieval. *Psychological Review, 85,* 59–108. http://dx.doi.org/10.1037/0033-295X.85.2.59

Ratcliff, R., & Rouder, J. N. (1998). Modelling response times for two choice decisions. *Psychological Science, 9,* 347–356. http://dx.doi.org/10.1111/1467-9280.00067

Redgrave, P., Rodriguez, M., Smith, Y., Rodriguez-Oroz, M. C., Lehericy, S., Bergman, H., . . . Obeso, J. A. (2010). Goal-directed and habitual control in the basal ganglia: Implications for Parkinson's disease. *Nature Reviews Neuroscience, 11,* 760–772. http://dx.doi.org/10.1038/nrn2915

Resulaj, A., Kiani, R., Wolpert, D. M., & Shadlen, M. N. (2009). Changes of mind in decision-making. *Nature, 461,* 263–266. http://dx.doi.org/10.1038/nature08275

Rizzolatti, G., & Luppino, G. (2001). The cortical motor system. *Neuron, 31,* 889–901. http://dx.doi.org/10.1016/S0896-6273(01)00423-8

Roitman, J. D., & Shadlen, M. N. (2002). Response of neurons in the lateral intraparietal area during a combined visual discrimination reaction time task. *The Journal of Neuroscience, 22,* 9475–9489. http://www.ncbi.nlm.nih.gov/pubmed/12417672

Santens, S., Goossens, S., & Verguts, T. (2011). Distance in motion: Response trajectories reveal the dynamics of number comparison. *PLoS ONE, 6,* e25429. http://dx.doi.org/10.1371/journal.pone.0025429

Schall, J. D., & Bichot, N. P. (1998). Neural correlates of visual and motor decision processes. *Current Opinion in Neurobiology, 8,* 211–217. http://dx.doi.org/10.1016/S0959-4388(98)80142-6

Schmidt, R., Leventhal, D. K., Mallet, N., Chen, F., & Berke, J. D. (2013). Canceling actions involves a race between basal ganglia pathways. *Nature Neuroscience, 16,* 1118–1124. http://dx.doi.org/10.1038/nn.3456

Schöner, G., & Thelen, E. (2006). Using dynamic field theory to rethink infant habituation. *Psychological Review, 113,* 273–299. http://dx.doi.org/10.1037/0033-295X.113.2.273

Shadlen, M. N., & Newsome, W. T. (2001). Neural basis of a perceptual decision in the parietal cortex (area LIP) of the rhesus monkey. *Journal of Neurophysiology, 86,* 1916–1936. http://dx.doi.org/10.1152/jn.2001.86.4.1916

Siegler, R. S., & Opfer, J. E. (2003). The development of numerical estimation: Evidence for multiple representations of numerical quantity. *Psychological Science, 14,* 237–243. http://dx.doi.org/10.1111/1467-9280.02438

Simon, H. A., & Newell, A. (1971). Human problem solving: The state of the theory in 1970. *American Psychologist, 26,* 145–159. http://dx.doi.org/10.1037/h0030806

Song, J.-H., & Nakayama, K. (2009). Hidden cognitive states revealed in choice reaching tasks. *Trends in Cognitive Sciences, 13,* 360–366. http://dx.doi.org/10.1016/j.tics.2009.04.009

Spivey, M. J., Grosjean, M., & Knoblich, G. (2005). Continuous attraction toward phonological competitors. *Proceedings of the National Academy of Sciences of the United States of America, 102,* 10393–10398.

Standage, D., You, H., Wang, D.-H., & Dorris, M. C. (2011). Gain modulation by an urgency signal controls the speed-accuracy trade-off in a network model of a cortical decision circuit. *Frontiers in Computational Neuroscience, 5,* 7.

Sternberg, S. (1966). High-speed scanning in human memory. *Science, 153,* 652–654. http://dx.doi.org/10.1126/science.153.3736.652

Sternberg, S. (1969). The discovery of processing stages: Extensions of Donders' method. *Acta Psychologica, 30,* 276–315. http://dx.doi.org/10.1016/0001-6918(69)90055-9

Sullivan, N., Hutcherson, C., Harris, A., & Rangel, A. (2015). Dietary self-control is related to the speed with which attributes of healthfulness and tastiness are processed. *Psychological Science, 26,* 122–134. http://dx.doi.org/10.1177/0956797614559543

Suminski, A. J., Mardoum, P., Lillicrap, T. P., & Hatsopoulos, N. G. (2015). Temporal evolution of both premotor and motor cortical tuning properties reflect changes in limb biomechanics. *Journal of Neurophysiology, 113,* 2812–2823. http://dx.doi.org/10.1152/jn.00486.2014

Swanson, L. W. (2012). *Brain architecture: Understanding the basic plan.* New York, NY: Oxford University Press.

Thura, D., Beauregard-Racine, J., Fradet, C.-W., & Cisek, P. (2012). Decision making by urgency gating: Theory and experimental support. *Journal of Neurophysiology, 108,* 2912–2930. http://dx.doi.org/10.1152/jn.01071.2011

Thura, D., & Cisek, P. (2014). Deliberation and commitment in the premotor and primary motor cortex during dynamic decision making. *Neuron, 81,* 1401–1416. http://dx.doi.org/10.1016/j.neuron.2014.01.031

Townsend, J. T. (1972). Some Results Concerning the Identifiability of Parallel and Serial Processes. *British Journal of Mathematical & Statistical Psychology, 25,* 168–199. http://dx.doi.org/10.1111/j.2044-8317.1972.tb00490.x

Townsend, J. T. (1976). Serial and within-stage independent parallel model equivalence on the minimum completion time. *Journal of Mathematical Psychology, 14,* 219–238. http://dx.doi.org/10.1016/0022-2496(76)90003-1

Townsend, J. T. (1981). Some characteristics of visual whole report behavior. *Acta Psychologica, 47,* 149–173. http://dx.doi.org/10.1016/0001-6918(81)90006-8

Townsend, J. T. (1990). Serial vs. parallel processing: Sometimes they look like Tweedledum and Tweedledee but they can (and should) be distinguished. *Psychological Science, 1,* 46–54. http://dx.doi.org/10.1111/j.1467-9280.1990.tb00067.x

Twomey, D. M., Murphy, P. R., Kelly, S. P., & O'Connell, R. G. (2015). The classic P300 encodes a build-to-threshold decision variable. *The European Journal of Neuroscience, 42,* 1636–1643. http://dx.doi.org/10.1111/ejn.12936

Vandekerckhove, J., & Tuerlinckx, F. (2008). Diffusion model analysis with MATLAB: A DMAT primer. *Behavior Research Methods, 40,* 61–72. http://dx.doi.org/10.3758/BRM.40.1.61

van Maanen, L., Fontanesi, L., Hawkins, G. E., & Forstmann, B. U. (2016). Striatal activation reflects urgency in perceptual decision making. *NeuroImage, 139,* 294–303. http://dx.doi.org/10.1016/j.neuroimage.2016.06.045

Van Opstal, F., Gevers, W., De Moor, W., & Verguts, T. (2008). Dissecting the symbolic distance effect: Comparison and priming effects in numerical and nonnumerical orders. *Psychonomic Bulletin & Review, 15,* 419–425. http://dx.doi.org/10.3758/PBR.15.2.419

Van Opstal, F., & Verguts, T. (2011). The origins of the numerical distance effect: The same–different task. *Journal of Cognitive Psychology, 23,* 112–120. http://dx.doi.org/10.1080/20445911.2011.466796

Verguts, T., Vassena, E., & Silvetti, M. (2015). Adaptive effort investment in cognitive and physical tasks: A neurocomputational model. *Frontiers in Behavioral Neuroscience, 9,* 57.

Weintraub, D. B., & Zaghloul, K. A. (2013). The role of the subthalamic nucleus in cognition. *Reviews in the Neurosciences, 24,* 125–138. http://dx.doi.org/10.1515/revneuro-2012-0075

Winter, C., Flash, S., Klavir, O., Klein, J., Sohr, R., & Joel, D. (2008). The role of the subthalamic nucleus in 'compulsive' behavior in rats. *The European Journal of Neuroscience, 27,* 1902–1911. http://dx.doi.org/10.1111/j.1460-9568.2008.06148.x

(Appendices follow)

Appendix A

Model Implementation and Optimization Procedure

Model Implementation

Premotor Cortex

Input units project to the PMd layer. In the current simulations, these input units may represent any task-relevant stimuli. For instance, a cue indicating that there is a high probability that the upcoming reach will be toward the left target would be strongly connected to the PMd left unit. In the following equations, activation of units in input, PMd, M1 layers are represented by the letters x, y, z, respectively. The activity of units in PMd is governed by the differential Equation (2):

$$\tau \frac{d}{dt} y_j(t) = -\alpha y_j(t) + \sum_i w_r x_i - y_k w_{inh} + Noise(t) \qquad (2)$$

where y represents PMd unit activation. The index on y indicates the laterality of the PMd unit (i.e., ipsilateral or contralateral), hence if $j = 1$, then $k = 2$ and vice versa. Index i ranges over input units, x_i is the activation of input unit i, and $w_i > 0$ is the connection weight between the unit i and the PMd unit. The symbol τ is the encoding time constant, α is a decay constant, and *Noise* is a Gaussian random variable with mean 0 and standard deviation 2.5. PMd units inhibit each other with strength w_{inh}; consistently, callosal inhibitory connections have been reported between PMd cortices (Marconi, Genovesio, Giannetti, Molinari, & Caminiti, 2003). By suppressing the irrelevant (least active) PMd unit (through lateral inhibition), the system also suppresses the contingent M1 activity. Such a mechanism is supported by human transcranial magnetic stimulation (TMS) studies, showing that stimulating the dorsal premotor cortex suppresses contralateral motor activation (Mochizuki, Huang, & Rothwell, 2004; Mochizuki, Terao et al., 2004). Moreover, Thura and Cisek (2014) observed that when PMd firing rate activity reaches its peak, contralateral M1 firing rate activity is suppressed.

Motor Cortex

The input for M1 units are given by Equation (3):

$$\tau \frac{d}{dt} z_j(t) = -\alpha z_j(t) + y_j - z_k W_{inh} + Noise(t) \qquad (3)$$

where z represents M1 unit activation. The j, k indexing system on z is the same as that used in Equation (2). All remaining parameters also have the same meaning as in Equation (2). Here, the activation value of ipsilateral PMd units is sent to their corresponding M1

unit through direct excitatory projections, as evidenced in several studies (for reviews see Dum & Strick, 2002; Luppino & Rizzolatti, 2000; Rizzolatti & Luppino, 2001). Interhemispheric inhibition between primary motor cortices has been observed in several studies (e.g., Di Lazzaro et al., 1999; Ferbert et al., 1992).

Subthalamic Nucleus

To dissociate what action to select from when to execute it, we implemented a brake on the motor system. The model STN implements a gate on movement that is modified online depending on the M1 dynamics. For this purpose, it computes the absolute value of the difference in activation between both primary motor cortices units:

$$\delta(t) = |z_1(t) - z_2(t)| \qquad (4)$$

where z represents the activation of M1 units. In turn, the STN decreases its activity via Equation (5):

$$\tau \frac{d}{dt} STN(t) = -w_{M1} \times \delta(t) + Noise(t) \qquad (5)$$

where w_{M1} represents the connection between M1 and STN. The gate function of the STN is subtended by the sigmoid function b:

$$b = \frac{1}{1 + e^{-k(\delta - STN)}} \qquad (6)$$

The movement vector is continuously updated as follows (see Figure 1A):

$$\frac{d}{dt} V(t) = (z_1 \times \vec{v}_1 + z_2 \times \vec{v}_2) * b \qquad (7)$$

where two vectors are each weighted by the activation value of the selectively tuned M1 units. Specifically, the vector associated to a left response (i.e., $\vec{v}_1 = \begin{bmatrix} -1 \\ +1 \end{bmatrix}$) is weighted by the activation value of the M1 L unit (i.e., z_1). In the same vein, the vector associated to a right response (i.e., $\vec{v}_2 = \begin{bmatrix} +1 \\ +1 \end{bmatrix}$) is weighted by the activation value of the M1 R unit (i.e., z_2).

If $k \gg 1$ in Equation (6), we can approximate Equation (7) as follows:

$$\begin{cases} V(t) = \text{constant} & \text{if } STN > \delta \\ V(t) = (z_l \times \vec{v}_1 + z_r \times \vec{v}_2) & \text{otherwise} \end{cases} \qquad (8)$$

Computer codes implementing our model in the three simulations can be downloaded at https://osf.io/j6vuy/.

(Appendices continue)

Model Optimization Procedure

Three parameters were optimized to best fit the empirical data, namely the initial value of STN, the encoding time τ and decay factor α. Best fit parameters were obtained through a "zoom lens" stepwise grid search over the parameter space. We first performed a grid search with a rather large step between parameters values. Once this procedure found a parameter set yielding the highest coefficient of determination between simulated and empirical data, we reproduced the grid search with smaller steps (same number as the prior search) around the previously found parameter values,

and so on until best fit parameters were obtained. The coefficient of determination value stemmed from linearly regressing the eight empirical ITs and MTs from Calderon et al. (2015) on the eight simulated ITs and MTs obtained with every combination of the three parameters (see above). Parameters were optimized in Simulation 2, and then reused in Simulation 3.

Simulation 1 assessed the effect of modifying the STN initial value. The data in Simulation 1 were therefore produced with a low and high initial STN value. Appendix B shows the parameter values for Simulation 1, 2, and 3. Furthermore, Appendix C displays the input-to-PMd connection weights in each simulation.

Appendix B

Parameters Value for Each Simulation

Parameters	Simulation 1	Simulation 2	Simulation 3
α	.5	.95	.95
τ	50	52	52
STN	.5 (low)-1.5 (high)	1.55	1.55
w_{inh}	.5	.5	.5
w_{M1}	1.5	1.5	1.5
k	10^7	10^7	10^7

Appendix C

Weight Matrix of Inputs to PMd R and L for Each Simulation

Visual stimulus	Connection weight to PMd R	Connection weight to PMd L
Simulation 1		
>	1	0
<	0	1
Simulation 2		
R	.8	.2
r	.6	.4
L	.2	.8
l	.4	.6
>	1	0
<	0	1
Simulation 3		
1	.1	.9
2	.2	.8
3	.3	.7
4	.4	.6
5	.5	.5
6	.6	.4
7	.7	.3
8	.8	.2
9	.9	.1